Formin2A Fluctuates with Vesicles and Precedes F-actin During *Physcomitrella patens* Polarized Growth

A Major Qualifying Project

Submitted to the faculty of

WORCESTER POLYTECHNIC INSTITUTE

In partial fulfillment of the requirements for the

Degree in Bachelor of Science

In

Biology and Biotechnology

By

Ellen Pierce

Approved:

Luis Vidali, PhD

Worcester Polytechnic Institute

Biology and Biotechnology

Project Advisor

TABLE OF CONTENTS

1 ABSTRACT

It has been hypothesized that myosin and other cell components are located on vesicles to organize the actin network during polarized growth. Using confocal microscopy and fluctuation cross correlation analyses, I investigated the association of class II formins with vesicles and F-actin in *Physcomitrella patens* caulonemal cells. I found that formin2A co-localized with both VAMP, a vesicle marker, and Lifeact, an F-actin probe. Furthermore, formin2A fluctuated in phase with VAMP, but preceded Lifeact, in agreement with the hypothesis.

2 ACKNOWLEDGEMENTS

This project would not have been accomplished without support along the way. I would like to thank Professor Vidali for being my advisor, and helping me from experiments to report writing. I would also like to thank Dr. Fabienne Furt for supporting me extensively, both inside the lab and with the final report. I would like to thank the head of microscopy, Vicki Huntress, for training me on the confocal microscope and helping with any problems that arose along the way. Finally, I would like to thank everyone in the Vidali lab for supporting me throughout the entire project, both technically and personally.

3 INTRODUCTION

3.1 POLARIZED TIP GROWTH IN EUKARYOTIC CELLS

Polarized growth is a type of cell growth that is localized to a confined area of the cell, rather than diffuse growth that exhibits even growth in all directions (Yoo et al.). Tip growth is a specialized type of polarized growth where the cell wall extension and deposition of materials is focused at one end of the cell (Smith). As a result, the cells exhibit an elongated shape. This type of growth can be seen in animal, fungal and plant cells. An example of fungal polarized growth is the expansion of the hyphae, or branching extender cells (Harris); (Hepler et al.). Neurons are examples of animal cells that can grow through tip growth. Several plant cells grow via tip growth, including rhizoids in algae, pollen tubes and root hairs in higher plants, and protonemal cells from bryophytes (Hepler et al.); (Palanivelu and Preuss). These specialized cells are important for specialized tasks that require such expansion, such as extending into the environment for nutrients or reaching towards the ovule of the plant to deliver the sperm(Hepler et al.).

3.2 *PHYSCOMITRELLA PATENS*

3.2.1 *P. patens* as a model organism

The specimen used in this MQP project was *Physcomitrella patens*, a type of moss that is commonly used in biological research. It is ideal for a model organism for several reasons. First, the moss is in a haploid stage for most of its life cycle, so there is only one copy of each chromosome (Cove et al.). This makes it easier to determine whether a mutation in a gene has an effect or not. By comparison, if a diploid plant contains a second allele that does not carry the

mutation, any deleterious effects could be masked. *P. patens* also has the ability to integrate exogenous DNA into its own genome via homologous recombination which allows for gene knock-ins and gene knockout strategies. In addition, RNA interference (RNAi) can be used to knock down genes, which is useful to study essential genes (Vidali et al.). Moreover, the full genome of *P. patens* has been sequenced, making genetic studies of the organism much simpler (Rensing et al.). Finally, it is an organism that grows well under laboratory conditions (Cove et al.). *P. patens* is easy to maintain and propagate, and it has a short period from spore germination to protonemal cells, of about a week.

3.2.2 Tip growth in *P. patens*

The first stage of growth in a *P. patens* spore is the protonemal stage, also called the filamentous growth stage. During this stage, *P. patens* produces two types of growing cells: caulonemata and chloronemata. Both types of cells grow via tip growth (Menand et al.); (Vidali and Bezanilla). Chloronemata contain a large amount of chloroplasts and are mainly involved in photosynthesis. Caulonemata have fewer chloroplasts, and are generally longer and thinner than chloronemata. There are no large organelles localized in or near the tip of the cell, which gives the visual effect of having a clear zone at the end of a more solid cell shank. Caulonemata are involved with substrate colonization and nutrient acquisition (Menand et al.). The first cells to differentiate during the protonemal stage are chloronemata, and after about four days, the new cells produced at the tips of the filaments start to differentiate and become characteristic of caulonemata.

3.3 CELLULAR COMPONENTS OF PLANT POLARIZED GROWTH

3.3.1 Actin

One of the most important cellular components in polarized growth is the actin cytoskeleton. Actin is also the most abundant protein in most eukaryotic cells. Actin is a highly conserved protein, comparable to the conservation level of histones (Lodish). An actin monomer contains two major domains with a nucleotide binding cleft between them. Actin exists in two forms: G-actin (globular), which is a monomer, and F-actin (filamentous) which is a polymer. In the cell, there is a dynamic equilibrium between the G-actin and F-actin. Actin filaments along with actin binding proteins form the cytoskeleton (Figure 1), which provides a framework for various cellular processes such as polarity and cell morphogenesis (Henty-Ridilla et al.).

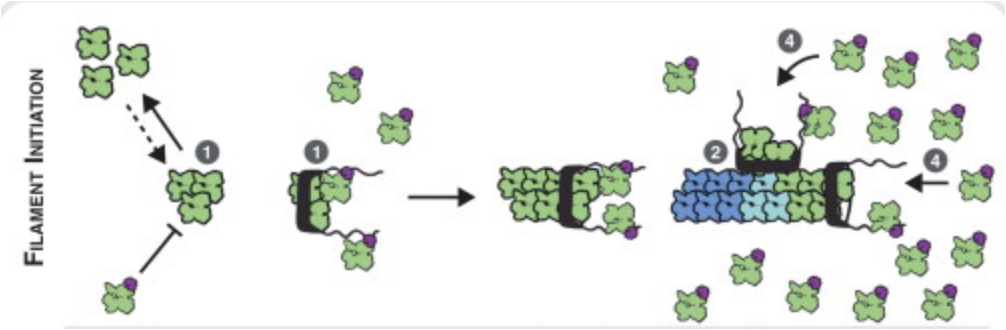

Figure 1: Visual of actin as both a monomer and a filament (Modified from (Henty-Ridilla et al.))

3.3.1.1 Actin in plants

Unlike animal cells, plant cells have a thick cell wall that prevents some of the actin dependent processes such as cell motility that are exhibited in animal cells. However, actin has other important functions within the plant cell. Many higher plant organelles use actin filaments for intracellular travel, such as mitochondria, Golgi bodies, and chloroplasts (Li and Nebenfuhr). In addition, actin filaments are involved in cell polarity, cell division, and polarized growth.

3.3.1.2 Actin in P. patens

Using an actin probe called Lifeact (Riedl et al.) fused with GFP, the dynamic actin network can be viewed in *P. patens* tip growing caulonemal cells under confocal microscopy (Vidali et al.). In addition to a rapidly remodeling (polymerizing and depolymerizing) network in the shank of the cell, there was also a small focal point localized at the very tip of the growing cell. However, Lifeact-mEGFP when overexpressed in *P. patens* negatively affects protonemal growth: fewer caulonemal cells grow and those that grow display a slower growth than their counterparts as well as those with a lower expression of Lifeact-mEGFP (Vidali et al.). The actin network in *P. patens* can be disrupted by the drug latrunculin B, which depolymerizes the actin filaments and has been shown to inhibit cell tip growth in the moss.

3.3.2 Myosin

Myosin is a motor protein that has the capability to move along actin filaments. Due to its ATPase activity, myosin converts the chemical energy of ATP hydrolysis to the mechanical energy necessary for the conformational changes that allow its movement. This activity is actin-activated, so only when the myosin is bound to actin will it experience this reaction.

There are approximately 35 classes of myosins (Maravillas-Montero and Santos-Argumedo). The three largest classes are myosin I, II, and V. Class V myosins, found in animals and fungi, has tail binding sites that correspond to plasma membranes or intracellular organelle membranes, so they carry out membrane-related activities (Trybus)such as transporting organelles, secretory vesicles, mRNA, and other cellular components. In animals, myosin Va is important for the nervous system and melanocytes. For example, lack of myosin Va causes defects in pigmentation, as well as neurological problems (Trybus).

3.3.2.1 Myosin XI

Myosin XI is the plant-specific homolog of myosin V. These two classes of myosins contain the same domain organization, with a head, a neck, a coiled coil domain, and a globular tail region (Li and Nebenfuhr). The head domain contains both actin and ATP binding sites. As a result, it binds to the actin and carries out the ATPase activity, which generates the force for movement. The neck domain contains 6 binding sites for calmodulin, connects the head and tail regions and regulates the activities of the head domain. The coiled-coil region between the neck and tail regions allows for dimerization of myosin proteins (Tominaga and Nakano). Finally, the tail domain contains binding sites that determine the specific function. For example, myosin XI tail domains may bind membranous organelles, such as the endoplasmic reticulum or Golgi stacks (Buchnik et al.). Myosin XI is responsible for cytoplasmic streaming and for large organelle transport in flowering plants as myosin V is for animals and fungi (Li and Nebenfuhr). Myosin XI is physically distinct from Myosin V in that it has a much shorter coiled-coil region but otherwise has head, neck, and tail domains of comparable size. The visualization of the two classes of myosins can be seen below in Figure 2 (Li and Nebenfuhr).

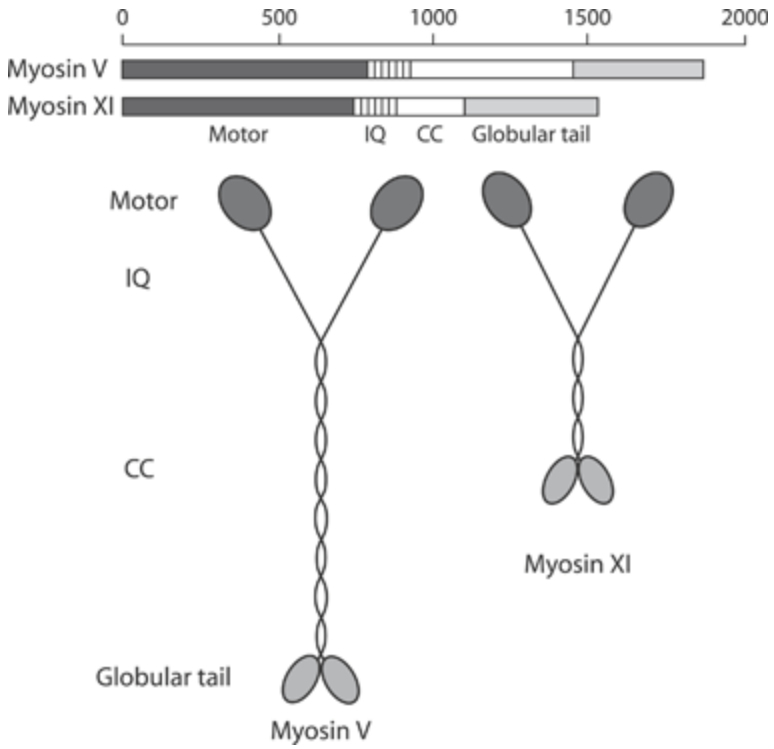

Figure 2: Visual Comparison of Myosin V and Myosin XI (Li and Nebenfuhr)

In plants, myosin XI has been shown to be necessary for cell development and growth. When myosin XI isoforms K and 2 were knocked out of *Arabidopsis* plants, the resulting plants had stunted overall growth, stunted leaf growth, stunted root hairs, and delayed flowering (Peremyslov et al.). The same study also showed that when the two myosin XI types (K and 2) were knocked out, Golgi stack and peroxisome motility significantly decreased. These findings support the theory on myosin XI's role in organelle transport within the plant cell (Peremyslov et al.).

A later study from the same lab suggests that myosin XI not only associated with the larger organelles, but also potentially smaller cellular components like vesicles. Peremyslov et al. (2012) fluorescently tagged the myosin XI-K isoform, and investigated its distribution in *Arabidopsis* cells. They discovered that this isoform localized to endomembrane compartments that are thought to be vesicles. The myosin XI-K was also found localizing to the tip of growing

root hairs, which grow via polarized growth. This indicates that myosin XI-K in *Arabidopsis* is important for polarized growth (Peremyslov et al.).

3.3.2.2 Myosin XI in P. patens

The *P. patens* genome contains two genes encoding myosin XI proteins, labelled a and b. The two versions have 94% identity, and are functionally redundant. Therefore, if one gene of myosin XI is nonfunctional, the moss shows no phenotypic effects and grows similarly to the wild type (Vidali et al.). In tip growing caulonemal cells, confocal microscopy revealed that myosin XIa localizes to the apex along with actin, forming a concentrated focal point at the tip. However, statistical analysis of the normalized fluorescence intensity of caulonemal cells containing fluorescently tagged myosin and actin showed that the myosin fluorescence fluctuated before actin did. In other words, myosin preceded actin at the growing cell tip. This suggests that the myosin XI in *P. patens* is involved in organizing the actin filaments, rather than the actin filaments determining where the myosin XI moves (Furt et al.). In the same study, it was also shown that myosin co-localized to the tip of the cell along with VAMP, a v-SNARE protein that is used as an endogenous vesicle marker. When the temporal relationship between the fluctuations was analyzed in the same manner as the myosin and actin, it was found that myosin and VAMP (vesicles) are fluctuating at the same time. This suggests that myosin XI in *P. patens* may be responsible for vesicle motility during tip growth (Furt et al.).

3.3.3 Rab proteins

Rab proteins are a family of highly conserved monomeric GTPases that help regulate organelle transport in eukaryotic cells. They have both an active stage (GTP-bound) and their inactive stage (GDP-bound), and are capable of regularly cycling between the two stages. Rab proteins are associated with several organelle functions, such as membrane docking, vesicle

budding, and vesicle motility (Zerial and McBride). They have been shown to activate effectors, which are factors that transduce the Rab proteins signal caused by the switch from one stage to another. Unlike the Rab proteins, the Rab effectors are not highly conserved. Rather, they appear to be specialized for each transport system (Zerial and McBride).

3.3.3.1 Rab proteins in plants

In plants, Rab proteins are known to be involved in organelle transport. *Arabidopsis* Rab proteins ARA6 and ARA7 have been found to localize to vacuolar membranes, and ARA6 also regulates SNARE complex formation at the plasma membrane (Ebine et al.);(Uemura and Ueda). Rab proteins are also shown to be related to plant tip growth. One study found that RabA4b in *Arabidopsis* localized to the tip of growing root hair cells, which grow by tip growth. This localization was disrupted after treatment with the actin depolymerizing drug latrunculin B, and this lack of localization was correlated to inhibited polarized growth. The researchers proposed that RabA4b is involved in membrane trafficking in *Arabidopsis* on a compartment that is important for polarized growth (Preuss et al.).

3.3.4 Formins

3.3.4.1 General Function

Formins are a large group of eukaryotic proteins that share a common domain called Formin Homology domain 2 (FH2). They were originally surmised to play a role in signaling and cytoskeletal organization, but recent experiments have provided more specific information. One of the most important discoveries found was that the FH2 domain of formins has the ability to nucleate and elongate actin (Cvrckova). Unlike an actin regulating protein complex (e.g. Arp 2/3 complex) that associates with the pointed end of an actin filament, formins extend the actin by first dimerizing around the barbed end of the filament (Cvrckova). They then sequentially

bind actin monomers using the FH2 domain. The dimer, as a "leaky" cap (allowing the filament to polymerize), "walks" with the barbed end of the actin filament. As a new actin monomer binds to the end of the actin filament, the actin monomer that had previously been the end of the filament releases from the FH2 domain of the formin and attaches to the new end of the filament (Zigmond).

3.3.4.2 Plant formins and their specific function

Studies have shown that, in general, plants have many different formin isoforms, grouped in three classes. Class I formins are integral membrane proteins and anchor the actin cytoskeleton at the cell cortex to the cell wall, while Class II formins serve as actin polymerization drivers (Cvrckova). Class II formins are normally characterized by their shared PTEN domain near the N-terminal of the protein, while Class I formins often contain a transmembrane domain. Class III formins are found only in lower plants like mosses and lycophytes. These formins contain a Rho GTPase activating protein domain (Figure 3). While the exact function of Class III formins has not been identified, it has been noticed that all plants containing these genes have flagellate sperm (van Gisbergen and Bezanilla).

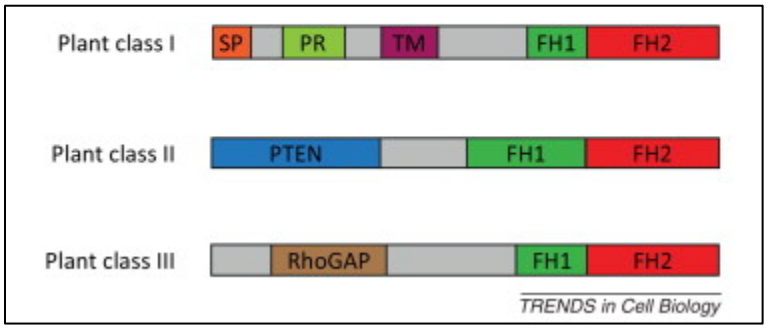

Figure 3: Comparison of the three distinct classes of plant formins (Modified from (van Gisbergen and Bezanilla))

Many of these isoforms have functions involving direct or indirect actin regulation (Cvrckova). For example, the class I AtFH1 isoform in *Arabidopsis* has been shown to cause actin bundling, and overexpression of this isoform can lead to cell tip swelling due to excessive amounts of actin filaments. Another *Arabidopsis* isoform, class II AtFH14, has demonstrated a role in cell division and meiosis by binding both actin and microtubules. Finally, a rice formin isoform (FH5) binds to microtubules, as well as nucleating and bundling actin. Its absence in a cell leads to organ bending and stunted cell growth, which would indicate that FH5 has a role in cell growth (Cvrckova).

3.3.4.3 Formins in Physcomitrella patens

The three classes of formins are present in *Physcomitrella patens*. Class II formins have been found in *P. patens* to localize to the growing cell tip (Vidali et al.); (van Gisbergen et al.). In *P. patens*, the PTEN domain of the class II formins has been found to be the cause of the localization to the tip. When only the PTEN domain was transformed into a wild type moss line with a 3mEGFP tag, the PTEN domain also localized to the apex of the cell tip (Vidali et al.). The PTEN domain has also been found to bind to a phosphoinositide, PI (3, 5) P2, using lipid overlay assays. The same study also showed that this binding to the PTEN domain is essential for polarized growth (van Gisbergen et al.) (Vidali et al.). It has been found that the two main classes of formins (Classes I and II) perform different tasks in the tip growing protonemal cells. Using RNAi, all the genes for one class of formin were silenced in a plant and any change in growth observed. The class I formins were not shown to be essential for polarized growth, while the class II formins were found necessary. However, the class I formins caused stunted plant growth without negatively affecting the rate of polarized growth. Because of this, it was suggested that the class I formins have a role in cell division (Vidali et al.).

3.4 PURPOSE OF THIS STUDY

The purpose of this MQP project is to study the interaction of formin2A with other cellular components such as myosin, actin filaments, and vesicles in *P. patens* caulonemal cells during tip growth. While it has been established that class II formins localize to the growing cell tip and are essential for polarized growth in *P. patens*, there have not been many studies examining the relationships between class II formins and the other essential components in polarized growth. The other reason to undertake this project is to support the recently proposed lab model. This model was proposed by (Furt et al.), and rather than a traditional model that shows myosin and vesicles running along preexisting actin filaments, the active model suggests that the vesicles contain on their membranes myosin and actin elongators such as formin2A to create actin filaments (Figure 4). While some research has been done to determine the validity of this model, more evidence is needed to support or disprove the model.

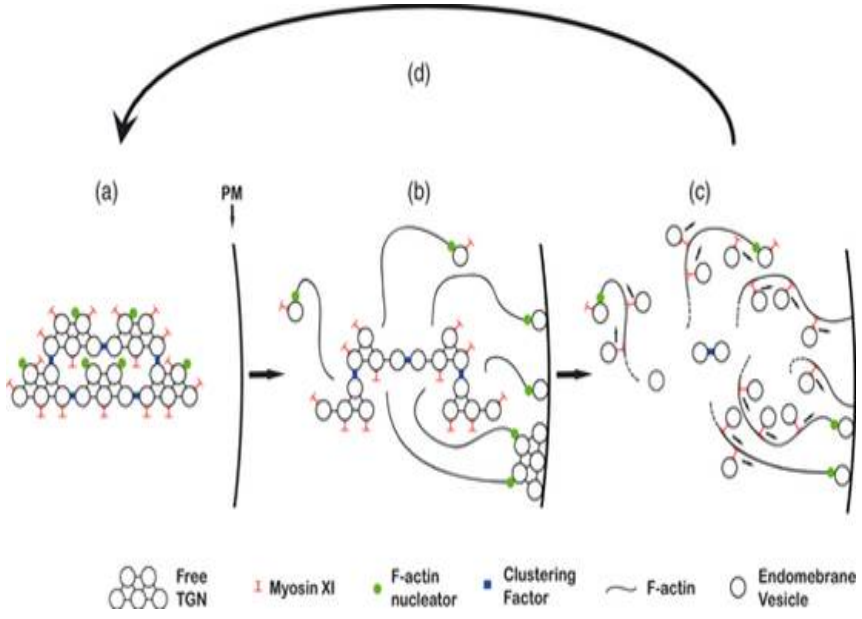

Figure 4: Active model for polarized growth as proposed by (Furt et al.)

There were two hypotheses involved with this study. Based off prior studies (Furt et al.), it was hypothesized that formin2A would fluctuate in phase with vesicles. It was also hypothesized that the formin2A levels would precede F-actin's. To achieve these goals, transformations of *P. patens* with the desired cellular component fused with a fluorescent protein such as GFP were performed to obtain stable cell lines expressing two components simultaneously tagged with two different fluorescent probes (3mEGFP, 3mCherry). Imaging of these lines helped to determine whether formin2A co-localizes with any of these components in the caulonemal clear zone using confocal microscopy. Analysis of the fluctuations of the fluorescence helped determine whether formin2A fluctuates at the same time as the cellular component, and if not which precedes the other. The expected results were that the data generated from this project would support the active model.

4 METHODOLOGY

4.1 MOSS PROPAGATION

The different moss lines used in this research were grown on cellophane on $PpNO_3$ or $PpNH_4$ medium containing 0.7% agar (w/v), and were propagated from week to week using the Vidali lab protocols. Briefly, one week-old moss tissue was scraped off the cellophane and placed into a culture tube along with 1 ml of water. A homogenizer was used to grind the moss and water mixture until any chunks of moss had been broken up. Finally, 700ul of the homogenized moss mixture were added on fresh $PpNO_3$ or $PpNH_4$ medium containing 0.7% agar (w/v). 300ul of the mixture were added on LB medium containing 1.5 % (w/v) agar, in order to determine whether any contamination by bacteria was present.

4.2 CLONING

4.2.1 LR Reaction

The LR reaction was performed using Gateway cloning protocol (Lifetechnologies). 1 µl of Clonase was added to the mixture of the two entry clones containing 3mCherry and VAMP respectively, and the destination vector pTKUbigate. The LR reaction was incubated at room temperature overnight. To stop the LR reaction, 0.5 µl of Proteinase K was added to the mixture, which was then incubated at 37°C for 10 minutes.

4.2.2 Digestion reaction

After the LR reaction had been performed, a digestion reaction had to be done in order to determine that the construct had been created properly. NheI and AflII were chosen as restriction enzymes because of the location of their corresponding restriction sites on the plasmid, with two

restriction sites flanking the inserts and one being in the middle of the insert. The final volume of the reaction was 20 µl. 2 µl of NE Buffer 4 (10X) and 0.2 µl of BSA (100X) (New England Biolabs) were added to a sterile 1.5 ml Eppendorf tube, along with 3 µl of construct DNA and 0.5 µl of each restriction enzyme. The final volume of the digestion reaction was adjusted to the 20 µl with distilled water. The reaction incubated for 2 hours at 37°C, and after was frozen in preparation for gel electrophoresis the next day.

4.2.3 *E. coli* transformation

An *E. coli* transformation was performed when plasmid DNA needed to be amplified. One aliquot of NEB 5-alpha *E. coli* competent cells (New England Biolabs) was taken out of a -80°C freezer and placed immediately on ice to thaw for about 5 minutes. 10 µl of the competent cells were transferred to a chilled Eppendorf tube using a pre-chilled tip. 0.2 µl of the plasmid mini-prep was added to the competent cells, and the mixture was incubated on ice for about 30 minutes. The cells were then subjected to heat shock (at 42°C in a water bath for 30 seconds), and put back on ice for another 5 minutes. 250 µl of liquid LB media were added to the cells, and the cells were incubated for an hour at 37°C under shaking. After the incubation, the transformed cells were plated on two selective media plates (LB+100 µg/ml Carbenicillin). These plates were incubated at 37°C for 16 hours or less, then removed, sealed, and placed in the fridge until colonies needed to be picked for mini or maxi preps.

4.2.4 Mini and Maxi Preps

Mini and maxi preps were used to isolate and purify plasmid DNA after it had been amplified by growing it in transformed *E. coli* bacteria. Nucleospin (Machery-Nagel) mini preps were used when there was a smaller amount of plasmid DNA to isolate, while NucleoBond Xtra (Machery-Nagel) maxi preps were used when there was a much larger amount. Predicted DNA

yield for a mini was 25-45 µg, and 1000 µg for a maxi. However, both followed similar procedures.

The mini prep required 2 ml of transformed *E. coli* culture to proceed. A colony was picked off the selective media plate and transferred to a tube containing 2 ml of sterile LB media + 100 µg/ml Carbenicillin. This starter culture was allowed to shake overnight for about 16 hours. Once the incubation period was over, the bacteria in each tube was transferred to 2 ml Eppendorf tubes and centrifuged at 11,000 g for 30 seconds to pellet the cells. The supernatant was discarded, and 250 µl of a resuspension buffer containing RNAse were added. The *E. coli* pellet was resuspended completely and then 250 µl of a lysis buffer were added. The mixture was inverted 8 times, and incubated for 5 minutes at room temperature. After the incubation 300 µl of a neutralizing buffer were added and the tube was inverted another 8 times. The tube was centrifuged at 11,000 g for 5 minutes to separate the supernatant from the cellular debris and the genomic DNA released by the lysis buffer. The supernatant was transferred from the tube into a Nucleospin column and collection tube and centrifuged at 11,000 g for 1 minute. The flow-through was discarded, 600 µl of a washing buffer was added to the column, and it was centrifuged again at 11,000 g for 1 minute. The flow-through was discarded and the column was placed back in the empty collection tube. The tube was centrifuged at 11,000 g for 2 minutes, and after the collection tube was discarded. The column was inserted into a clean 1.5 ml Eppendorf tube, 50 µl of elution buffer was added to the column, and the tube was centrifuged for 1 minute at 11,000 g to collect the purified DNA. Afterwards, the column was discarded and the Eppendorf tube was labelled and stored at -20°C. To measure the concentration of plasmid DNA, part of the product in the Eppendorf tube was diluted 1/10 and measured on a Nanodrop machine, which measured the concentration of nucleic acids in the sample.

Unlike the mini prep, the maxi prep needed a large amount of *E. coli* culture. A 2 ml starter culture was obtained by inoculation with one colony and was grown in the same manner as for the mini prep. After the incubation period, however, the full starter culture was added to 250 ml of sterile Terrific media (Sigma-Aldrich) supplemented with 100 µg/ml Carbenicillin. The culture was incubated on a shaker for another 16 hours. After this second incubation period, the contents of the flasks were transferred to 250 ml plastic Nalgene bottles, and centrifuged at 5,000 g for 30 minutes. The supernatant was discarded, leaving the *E.coli* pellet, and 12 ml of a resuspension buffer were added. The pellet was resuspended, and 12 ml of a lysis buffer were added. The bottle was gently inverted for about 5 times, and the mixture was incubated at room temperature for 5 minutes. After the 5 minutes 12 ml of neutralization buffer was added and the bottle was inverted about 10 times. The mixture was centrifuged at 5,000 g for 10 minutes. While the bottle was centrifuging, a Nucleobond column and column filter were set up on a stand and 25 ml of equilibration buffer were applied around the rim of the filter, wetting the entire area.

After centrifuging, the supernatant in the bottle was removed and applied around the rim of the column filter. The column was allowed to empty, and then 15 ml of the equilibration buffer was applied to the column filter and the column was allowed to empty. After this step, the filter was removed. 25 ml of a washing buffer was added to the column, and after the column had emptied, 15 ml of elution buffer were added. The eluate was collected in a 50 ml Falcon tube, and 10.5 ml of room temperature isopropanol were added to the tube. After vortexing vigorously, the tube was centrifuged at 7,500 g for 1 hour, and the supernatant was discarded. 5 ml of room temperature 70% (v/v) ethanol were added, and the tube was centrifuged at 7,500 g for 10 minutes. After removing as much ethanol from the tube without disturbing the pellet, the

remaining ethanol was allowed to evaporate from the tube under the hood. After all the ethanol was evaporated, 500 µl of sterile TE buffer were added, the pellet was resuspended, and the tube was stored at -20°C. To measure the concentration of plasmid DNA, part of the product in the tube was diluted 1/100 and measured on a Nanodrop machine, which measured the concentration of nucleic acids in the sample.

4.3 SwaI Digestion

The SwaI digestions were carried out in order to linearize plasmid DNA for greater transformation efficiency. The digestion reaction was carried out by mixing 60 µl of 10X NEB buffer 3, 6 µl of 100X BSA, 120 µg of DNA, and 10 µl of (10,000 units/ml) SwaI (NEB Biolabs). The final volume of the digestion reaction was adjusted to 600 µl with distilled water. The digestion reaction was incubated for 4 hours at room temperature. 60 µl of sodium acetate were added to stop the digestion, and half the amount of liquid in the tube was decanted into a second tube. 800 µl of ethanol absolute were added to each tube, and they were incubated at -20°C for 30 minutes. The tubes were then centrifuged at top speed (21000 g) for 5 minutes, and the supernatant was removed. A whitish pellet of DNA was seen in the tube at this stage. 500 µl of 70% (v/v) ethanol were added to each tube and they were centrifuged again at top speed (21000 g) for 5 minutes. After removing the supernatant, the tubes were left to air dry under sterile conditions. Once all ethanol had evaporated from the tubes, each pellet was resuspended in 50 µl of TE buffer (10 mM Tris-HCl, 1 mM disodium EDTA). The tubes were then incubated for 10 minutes at 37°C. Finally, the contents of the two tubes were combined into one tube and were stored at -20°C.

4.4 STABLE MOSS TRANSFORMATION

Moss transformation was carried out using the polyethylene glycol-mediated transformation protocol (Liu and Vidali). In a sterile empty Petri dish, 9 ml of 8% (w/v) mannitol and 3 ml of 2% (w/v) Driselase were mixed together (see Appendix A for composition). For reference, the Driselase is a mixture of three enzymes that break down plant cell walls (Sigma Aldrich). 5-7 days-old moss tissue, from the line to be transformed, was scraped off the cellophane using a sterile spatula, added to the mannitol and Driselase mixture, and put on a shaker at low speed for 1 hour. After the hour, the moss/mannitol/Driselase mixture was filtered through a 70 μm size sterile cell strainer (Fisher Scientific) into a sterile test tube to separate the moss cells lacking cell walls (called protoplasts) from the clumps of cells that still have cell walls. The protoplasts were centrifuged at 250 g for 5 minutes. The supernatant was discarded in a waste container, and 10 ml of 8% (w/v) mannitol were added to resuspend the protoplasts. After two supplemental washing steps, protoplasts were resuspended in 10 ml of 8% (w/v) mannitol. A cover-slip was placed on a haemocytometer, and 10 μl of the resuspended protoplast solution was pipetted between the cover-slip and the haemocytometer. Using a light microscope, the amount of protoplasts in each of the four large squares of the haemocytometer was counted. A visual of a large haemocytometer square can be seen below in Figure 5. The numbers of protoplasts counted on the four squares were averaged. In order to get the estimated amount of protoplasts in the tube, the average number of protoplasts was multiplied by ten thousand to get the estimated amount of protoplasts in 1 ml of the solution because the volume of each square on the haemocytometer is equal to 1/10,000 ml. Since there were 10 ml total in the tube, the number gained in the previous calculation was multiplied by ten. This was the estimated total number of protoplasts in the solution, which would be needed in the next step.

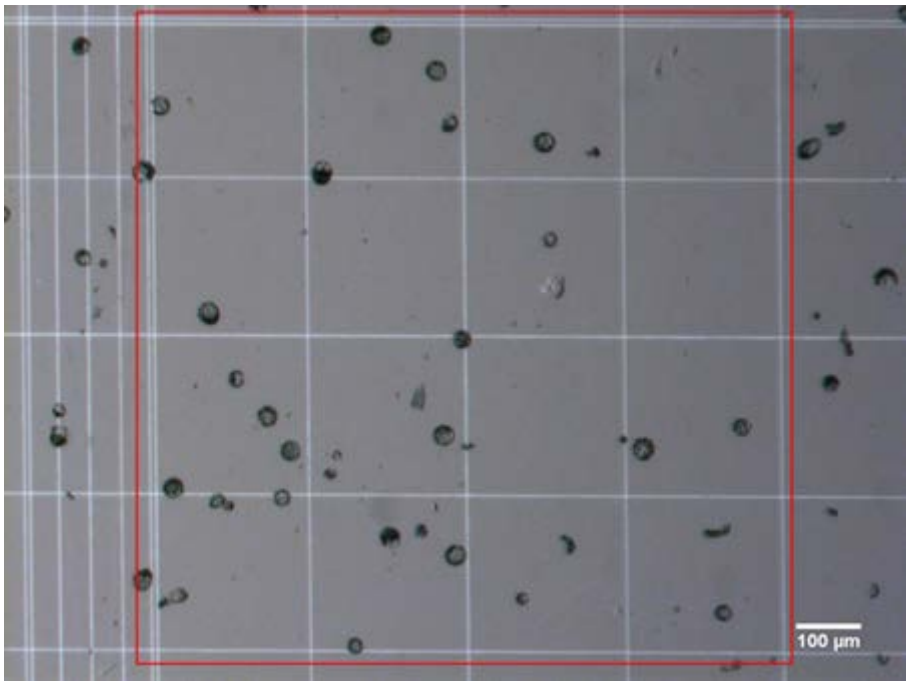

Figure 5: Visual of protoplasts on a haemocytometer square (Liu and Vidali)

Protoplasts were centrifuged one more time and resuspended in MMG buffer (for compositions see Appendix A) at a final concentration of 1.6 x 10^6 protoplasts per ml of buffer. Protoplasts were incubated in MMG buffer for 20 minutes at room temperature. After the incubation period, ~ 60 µg of SwaI digested-DNA (it was generally assumed that about half of the original 120 µg of DNA used in the digestion had been degraded) were added to 600 µl of resuspended protoplasts and mixed gently. 700 µl of polyethylene glycol (PEG) were then added to start the transformation. The transformation reaction was incubated for 30 minutes at room temperature. During this incubation period, 2 PRMB media plates were labelled and covered with cellophane (for composition of PRMB see Appendix A). The PRMT media was also melted and placed on a heating block (for composition of PRMT see Appendix A). After the incubation, the protoplasts were diluted with 3 ml of W5 and centrifuged at 250 g for 5 minutes in order to dilute the PEG (for composition of W5 see Appendix A). The supernatant was discarded into the waste container, and the transformed protoplasts were resuspended in 2 ml of warm PRMT

media. 1 ml of the resuspended protoplast solution was plated on each PRMB plate. Once the protoplasts had been spread through the entire plate, each plate was sealed with surgical tape (Micropore), and the plates were placed in the 25°C growth chamber.

After 4 days growing on the PRMB medium, the cellophane was transferred to a selective media plate (50 mg/ml Hygromycin). After a week, the cellophane was transferred to a fresh $PPNH_4$ plate. After another week, the cellophane was transferred back to a selective media plate (50 mg/ml Hygromycin). Finally, any surviving plants were individually picked and transferred sterilely to a new selective media plate without cellophane, also called a master plate (50 mg/ml Hygromycin) and allowed to grow for a week. Any green and growing plants were expanded into distinct lines.

4.5 SAMPLE PREPARATION FOR FLUORESCENCE SCREENING

"Sandwiches" were prepared by dispensing 100 µl of melted $PpNO_3$ medium onto a slide in order to create an evenly flat agar patch. Tissue from one week-old moss lines were placed on the agar patch. 10 µl of liquid $PpNO_3$ medium were then added on top of the agar patch and covered with a coverslip. The corners and edges of the coverslip were then sealed with melted VaLoP (1:1:1 Vaseline, lanolin, paraffin) and the slide was labeled for identification purposes.

4.6 SAMPLE PREPARATION FOR FLUCTUATION CROSS CORRELATION ANALYSIS

“Holey” slides (Mat Tek) were used for the purposes of performing intensity fluctuation analysis on any desired lines. These specialized small petri dishes with a coverslip attached at the bottom were sterilized and placed opened inside the hood. Sterile 1000 µl pipette tips were placed in the center of the dishes, wide end down. 5 ml of melted $PpNO_3$ media with 0.7% (w/v) agar were added into each dish around the pipette tips and allowed to solidify. Once the media

had solidified, the pipette tips were removed, leaving a hole in the media. 60-80 µl of melted $PpNO_3$ media with 0.7% (w/v) agar were added into the clear zone in the middle of the dish, creating a very thin media pad right on top of the coverslip. Finally, moss tissue previously grown on $PpNO_3$ media, was transferred to the center of the thin media pad in the center of the hole and was allowed to grow in the growth chamber for 7-12 days before being used for fluctuation analysis.

4.7 CONFOCAL MICROSCOPY

Confocal microscopy was used for the purpose of screening potential lines for fluorescent expression, as well as for the intensity fluctuation analysis undertaken on the lines determined to have the best fluorescent expression.

4.7.1 Fluorescence screening

Screening was done on any individual plants (lines) grown in the master plate that survived the two rounds of antibiotic selection and showed healthy growth. The plants were then grown on $PpNO_3$ (0.7% (w/v) agar) media for one week. Sandwiches were made of the lines based off the protocol listed previously. Using a Leica SP5 confocal microscope, the argon (25%) and 561 lasers were used to excite the 3mEGFP and 3mCherry fluorescent probes, respectively. The visible laser emissions were adjusted to 20% for 488 nm and for 561nm. The 63x oil objective N.A. 1.4 was used, and the emission filter ranges were set to 499-546 nm for 3mEGFP, and 574-646 nm for 3mCherry. The pinhole was set to 1AU. 5 caulonemal cells were randomly imaged at a resolution of 512x256 pixels with a zoom of 6, and their gain numbers for 3mEGFP and 3mCherry were recorded. A 10 minute video with images taken every 2 seconds was also taken of the 5th cell to ensure that the cells were growing.

4.7.2 Intensity fluctuation analysis

The confocal microscope was also used for the purposes of performing intensity fluctuation analysis on the lines that had been validated for the expression of both the 3mEGFP and 3mCherry fluorescent tags during the screening process. The settings were similar to the screening settings with two exceptions. The first was that the pinhole was all the way open at 6AU to collect the maximum light. In order to keep the cells from being overexposed to the laser and photobleaching the fluorescence, the visible emissions were decreased to 8% for the 488 nm and 6% for 561 nm. Because the movies involve 3 dimensional z stacks, an additional setting for the number and size of slices had to be added. For these tests, 9 slices at 1 um interval, were imaged. The movie was run at a resolution of 1028x256 pixels, with a zoom of 3. Stack images were collected every 5 seconds for 1 hour. After the movie was taken, an average projection of each stack was performed, compressing the 9 slices taken in each stack to 1.

4.7.3 Fluctuation cross-correlation analysis

Fluctuation cross correlation analysis was the method used in order to process the average projections from the movies. Using ImageJ software, the average projections were split into the two color channels, corresponding to the 3mEGFP and 3mCherry probe signals. A time projection image showing the maximum fluorescence was created for each channel, showing the fluorescence at the cell tip over the entire time period. An example of this can be seen below in Figure 6.

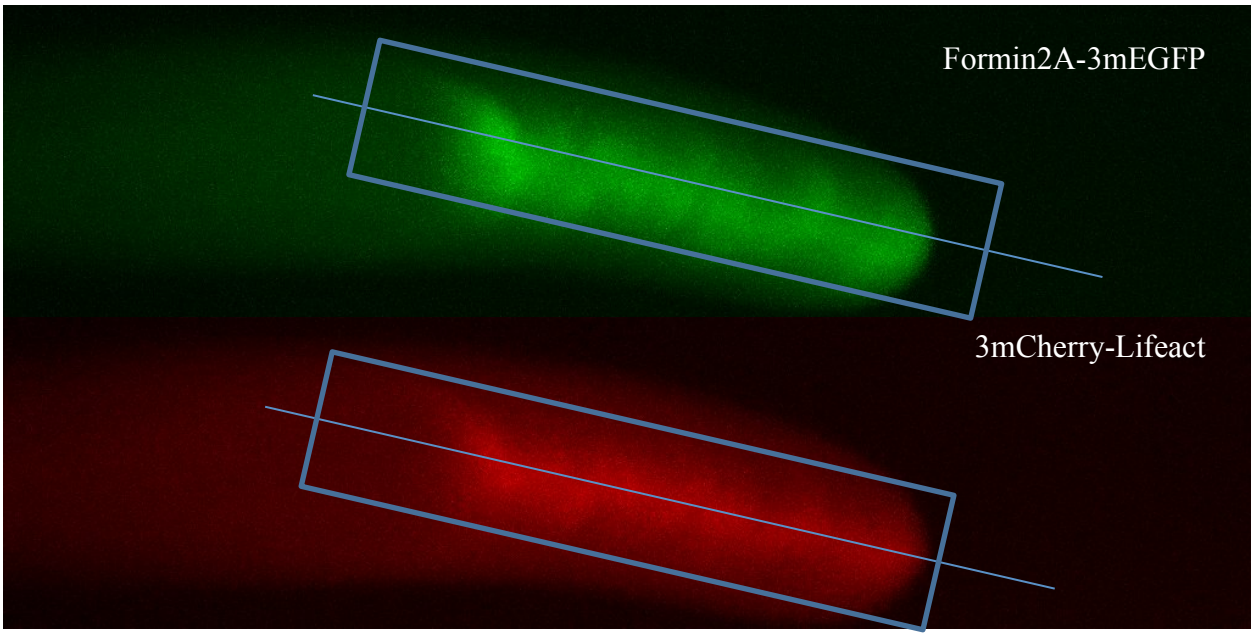

Figure 6: Paired images of maximal time projection. Examples of 61 pixel lines are shown overlaying the maximal time projects.

A line 61 pixels in width was traced on the time projection for each color channel from inside the shank of the cell through the tip, ending beyond the tip. The 61 pixel line was copied from the time projection image and pasted onto the original average projection movie. Using a MultipleKymograph plugin, a kymograph was created from the 61 pixel line on the average projection movie that showed the normalized intensity values of the fluorescence of both the cell tip and shank. The intensity values were normalized by subtracting the background fluorescence and dividing by the fluorescence in the shank of the cell. The normalized intensity values were then plotted in function of time. A kymograph was created by plotting the normalized intensity over time for each color channel, so one average projection movie would produce two total kymographs, one each for 3mEGFP and 3mCherry. An example of a kymograph can be seen in Figure 7.

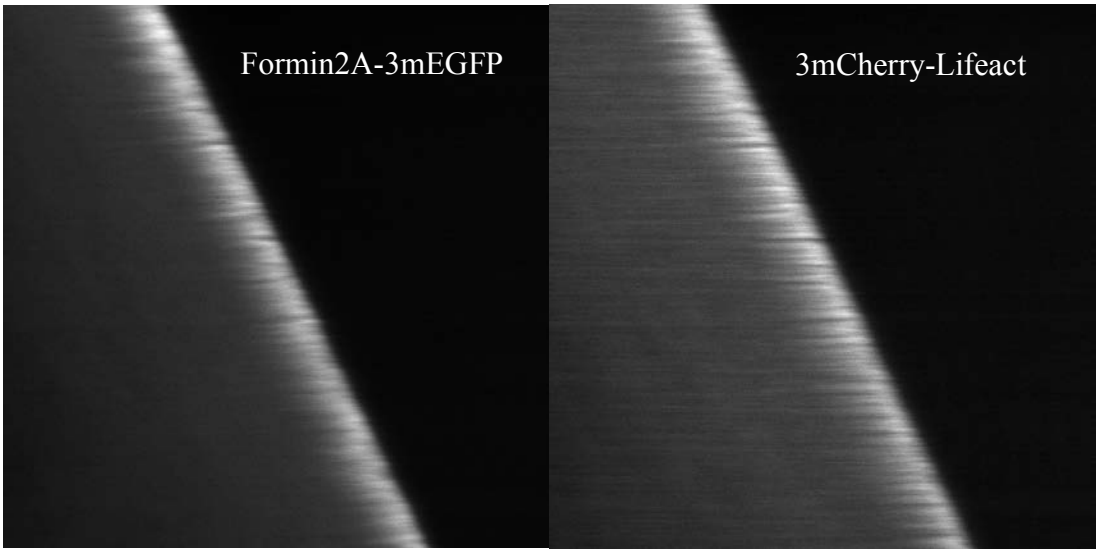

Figure 7: Kymographs for Formin2A-3mEGFP+ 3mCherry Lifeact cell

Once the kymographs had been created, they were run through an XCORR Matlab program containing a Fourier series detrending algorithm that compared the intensities of the two fluorescent tags to one another over all time points. The time difference corresponding to the maximum correlation coefficient between the two signals was determined by keeping one signal fixed and shifting the other one for each time point. The results were then plotted on a correlation coefficient vs. time shift (in seconds) graph. .

5 RESULTS

5.1 VAMP AND FORMIN2A LOCALIZE TO THE SAME REGION

In order to determine the relationship between formin2A and vesicles, a pre-existing Formin2A-3mEGFP moss line was transformed with a 3mCherry-VAMP, a vesicle marker. 5 promising lines were screened out of this transformation, and 3 were found to express both fluorescent markers (Appendix B). A line was considered good if both fluorescent markers were visibly expressing, and if the gains measured for each color channel was between 700 and 900. In addition, all of the cells tested should be expressing at similar levels. Using confocal microscopy to screen the 3 lines, it was found that VAMP and formin2A localize to the same apical region of the caulonemal cell (Figure 8).

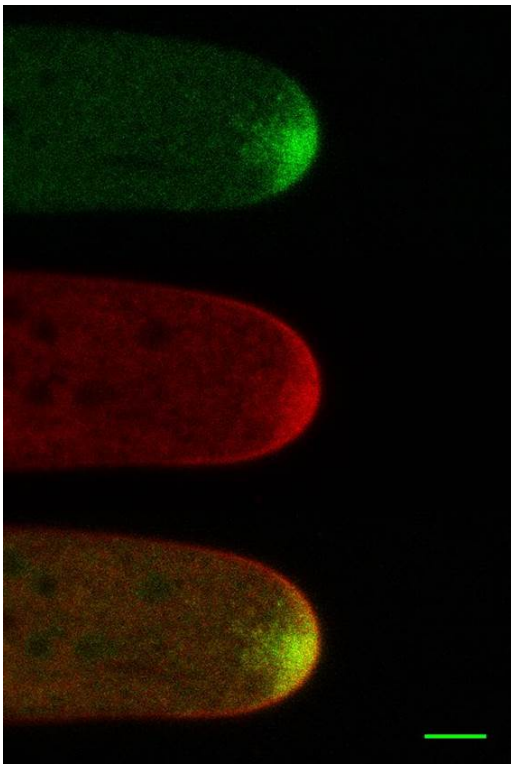

Figure 8: Localization of VAMP and Formin2A at the tip of a growing cell. Images of one transgenic line expressing Formin2A-3mEGFP (upper panel) + 3mCherry-VAMP (middle panel) acquired by confocal microscopy. The merged image is shown in the lower panel with Formin2A in green and VAMP in red. Scale bar = 5 µm

The cell shown in the above figure displays formin2A and VAMP expression at the tip of the cell. The formin2A shows a slightly larger spot, reaching back towards the shank of the cell. The VAMP (vesicle) fluorescence is showing a smaller spot at the tip, but also shows expression at the plasma membrane of the tip, causing a halo-like effect. The merged picture shows a large yellow spot where the two fluorescent tags overlap. This indicates that the two are co-localizing to the same apical region of the cell. This result is consistent with literature that showed that both formin2A and VAMP (vesicles) localize to the tip of a growing cell (Vidali et al.) (Furt et al.). The lines determined to be the best for testing were lines 19 and 28 (database numbers 807 and 809 respectively). Both had the two fluorescent markers expressing, with gains between 700 and 900. All cells tested were expressing the markers at similar levels, indicating homogenous lines.

5.2 VAMP IS IN PHASE WITH FORMIN2A

In order to further characterize the spatial and temporal relationships between formin2A and VAMP, 7 movies were taken of actively growing cells from the two best lines using confocal microscopy. An example of movie frames can be seen in Figure 9.

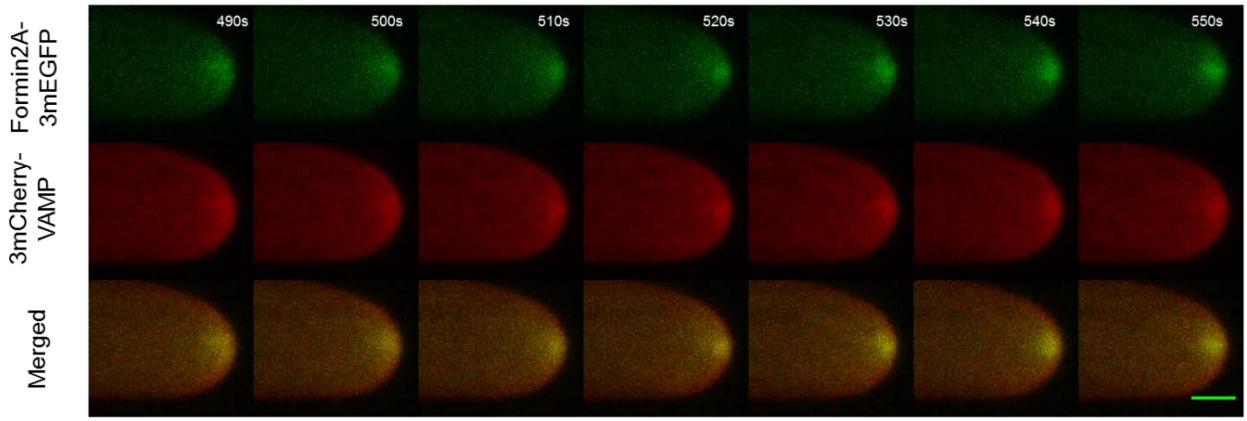

Figure 9: Time series of fluorescence intensity of Formin2A and VAMP at the cell tip. Average projections of Z-stacks acquired by confocal microscopy; scale bar = 5 µm

These frames demonstrate that the intensity of the fluorescence at the cell tip is fluctuating over time. In addition, the size of the fluorescent spot changes over time. At 490 s, the spot is faint and spread over most of the cell tip. However, by 530 s, the spot is showing greater intensity and has shrunk to a small focal point at the very tip of the cell.

The images from each movie were then run through a Fourier detrending algorithm in Matlab. The fluorescence intensity at the tip of the cell was normalized by subtracting the background fluorescence and dividing the fluorescence at the shank of the cell. The results of the normalized fluorescence intensity over time for an example cell can be seen below in Figure 10 and 11.

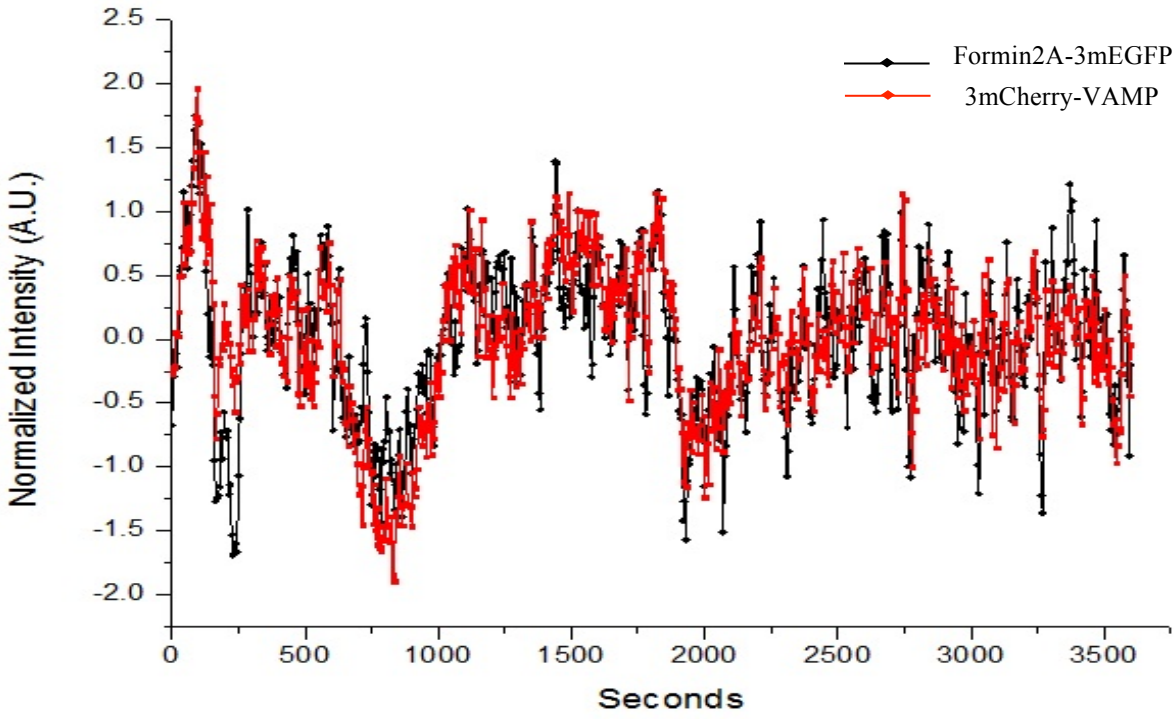

Figure 10: Normalized intensity of Formin2A-3mEGFP and 3mCherry-VAMP over time at the cell tip. Time points were acquired every 5 seconds

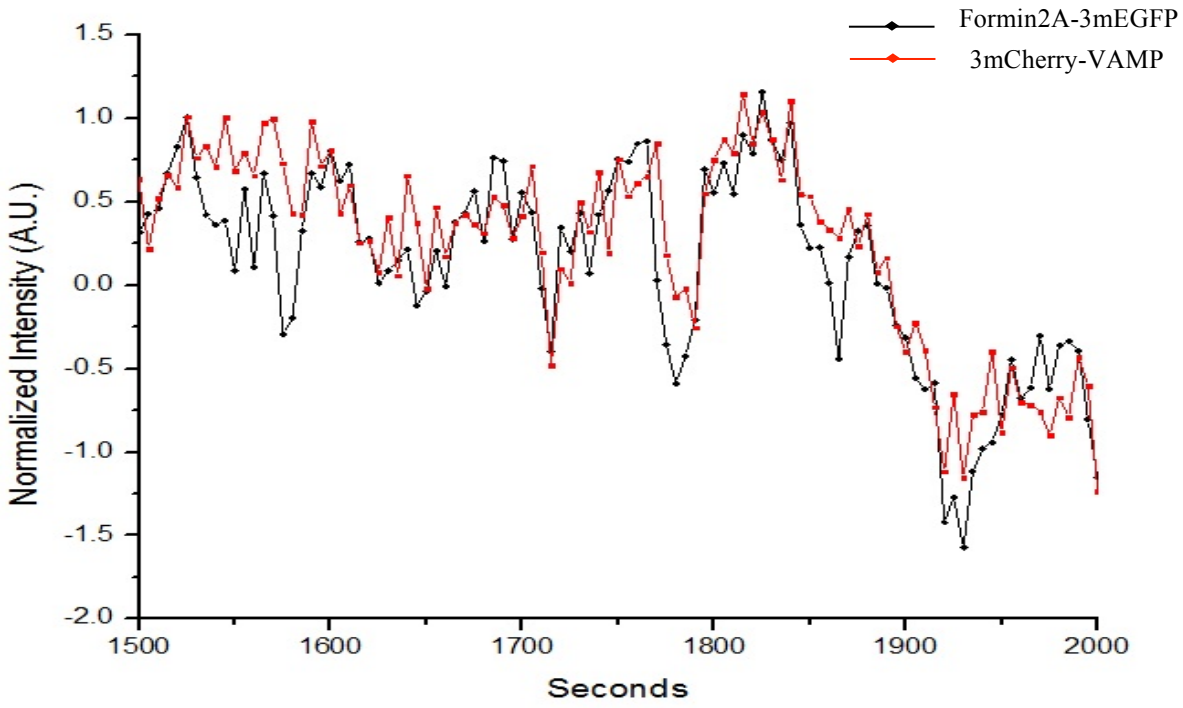

Figure 11: Zoom of the normalized intensity of Formin2A-3mEGFP and 3mCherry-VAMP over time at the cell tip. (1500-2000 second time frame from Figure 10)

These two figures confirm that the fluorescence intensity varies rapidly over time as shown in Figure 9. The formin2A (black) appeared to have fluctuations with larger amplitudes, often peaking above or falling below those recorded for VAMP (red). These results also show that the formin2A and the VAMP appear to be fluctuating more or less at the same time. However, it could not be confirmed using these graphs. In order to determine the exact temporal relationship between formin2A and VAMP, the intensities of the two fluorescent tags over all time points were compared to one another. Using another program in Matlab, the time difference corresponding to the maximum correlation coefficient between the two signals was determined by keeping one signal fixed and shifting the other one for each time point. A time difference close to 0 indicates that the signals are fluctuating in phase. The average result of all 7 cells tested can be seen below in Figure 12.

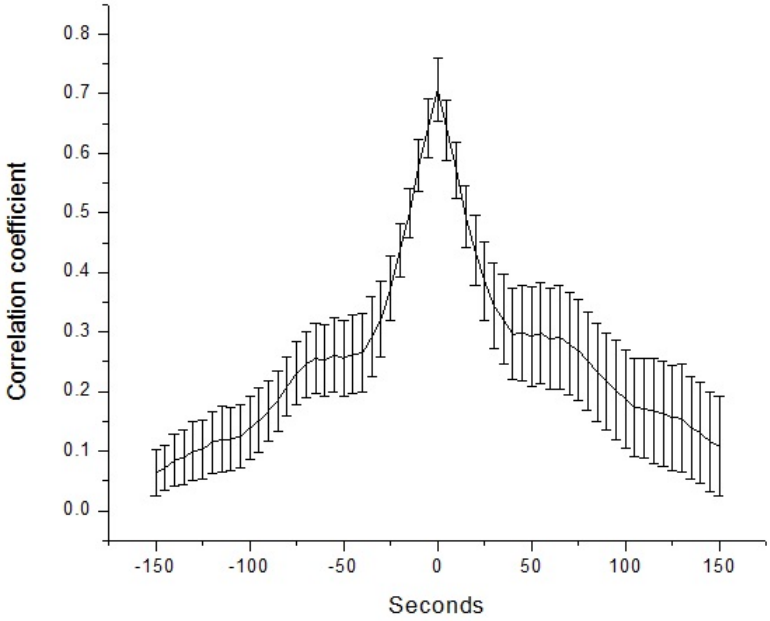

Figure 12: Cross-correlational analysis of VAMP vs. Formin2A phase. N=7; error bars are SE of the mean.

The graph is showing the correlation coefficient values for each time shift, with a range of -150 to 150 seconds. The maximum correlation coefficient shows a time shift of 0, indicating that VAMP and formin2A fluctuate at the same time at the cell tip during polarized growth.

5.3 F-ACTIN AND FORMIN2A LOCALIZE TO THE SAME REGION

In order to determine the relationship between formin2A and actin, a pre-existing Formin2A-3mEGFP moss line was transformed with LAMC (3mCherry-Lifeact), an F-actin marker. Four promising lines were screened from two transformations, and one was found to express both fluorescent markers. A line was considered good if both fluorescent markers were visibly expressing, and if the gains measured for each color channel was between 700 and 900. In addition, all of the cells tested should be expressing at similar levels. Using confocal microscopy to screen the lines, it was found that Lifeact and formin2A localize to the same apical region of the caulonemal cell (Figure 13).

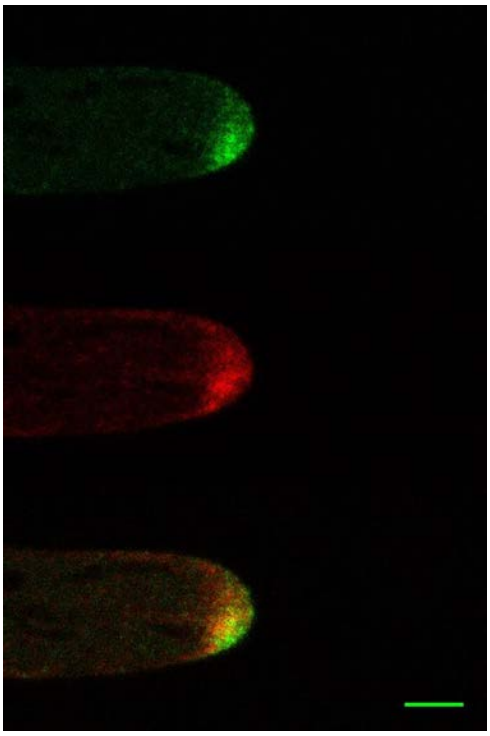

Figure 13: Localization of actin and Formin2A at the tip of a growing caulonemal cell. Images of one transgenic line expressing Formin2A-3mEGFP (upper panel) + 3mCherry-Lifeact (middle panel) acquired by confocal microscopy. The merged image is shown in the lower panel with Formin2A in green and Lifeact in red. Scale bar = 5 µm

The cell shown in the above figure displays formin2A and F-actin (Lifeact) expression at the tip of the cell. The formin2A shows a slightly stronger spot. The Lifeact (actin) fluorescence is showing a smaller spot at the tip, and is slightly fainter. The merged picture shows a yellow spot where the two fluorescent tags overlap. This indicates that the two are localizing to the same apical region of the cell. The line determined to be the best for testing was line 1 (database number 835). It had the two fluorescent markers expressing, with gains between 700 and 900. All cells tested were expressing the markers at similar levels, indicating homogenous lines.

5.4 FORMIN2A ANTICIPATES F-ACTIN

In order to further characterize the spatial and temporal relationships between formin2A and Lifeact, 6 movies were taken of actively growing cells from the two best lines using confocal microscopy. An example of movie frames can be seen in Figure 14.

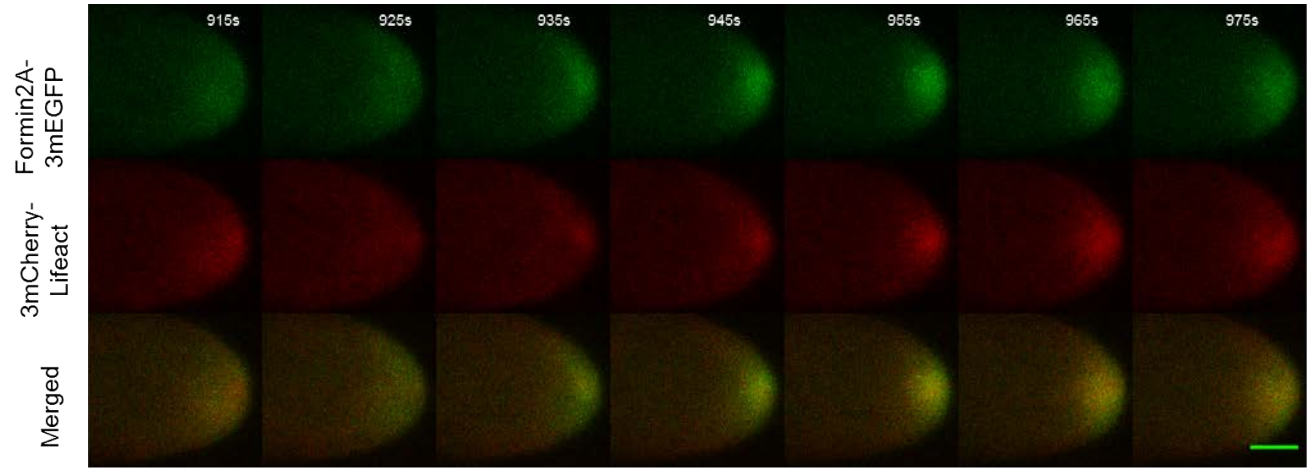

Figure 14: Time series of fluorescence intensity of Formin2A and VAMP at the cell tip. Average projections of Z-stacks acquired by confocal microscopy; scale bar = 5 µm

These frames demonstrate that the intensity of the fluorescence at the cell tip is fluctuating over time. In addition, the size of the fluorescent spot changes over time. At 915s, the spot is extremely faint and spread over most of the cell tip. However, by 945s, the spot is showing much greater intensity and has concentrated to a small focal point at the very tip of the cell.

The images from each movie were then run through a Fourier detrending algorithm in Matlab. The fluorescence intensity at the tip of the cell was normalized by subtracting the background fluorescence and dividing the fluorescence at the shank of the cell. The results of the normalized fluorescence intensity over time for one cell can be seen below in Figure 15 and 16.

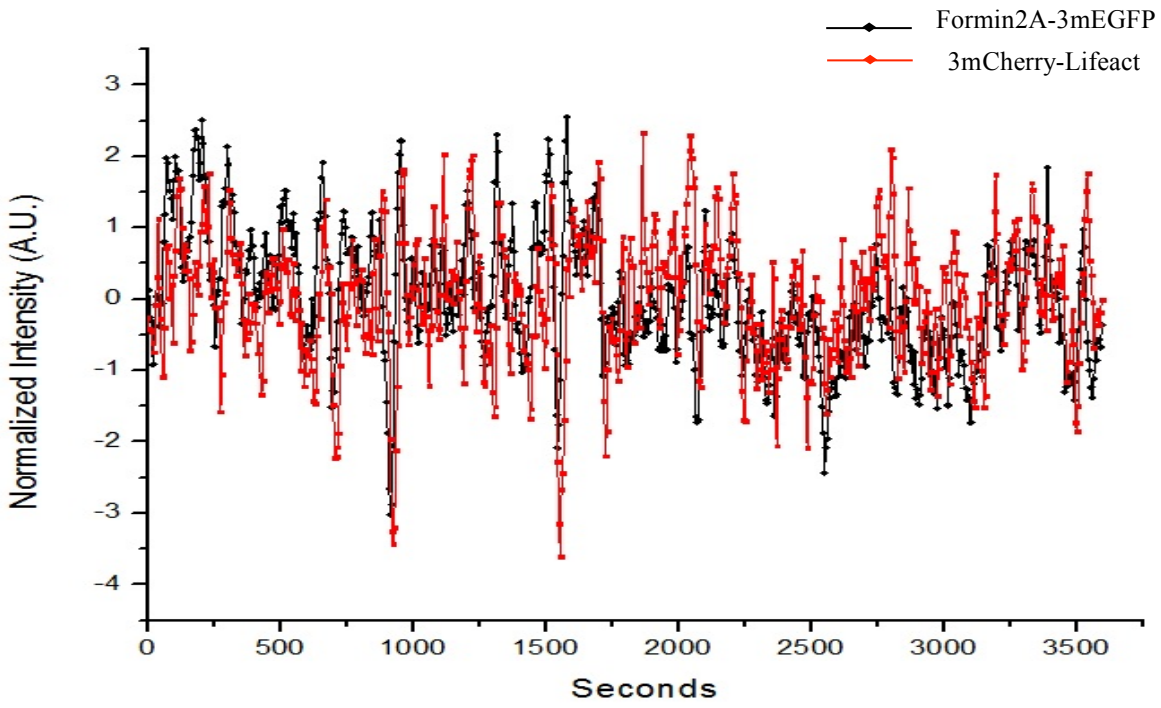

Figure 15: Normalized intensity of Formin2A-3mEGFP and 3mCherry-Lifeact over time at the cell tip. Time points were acquired every 5 seconds

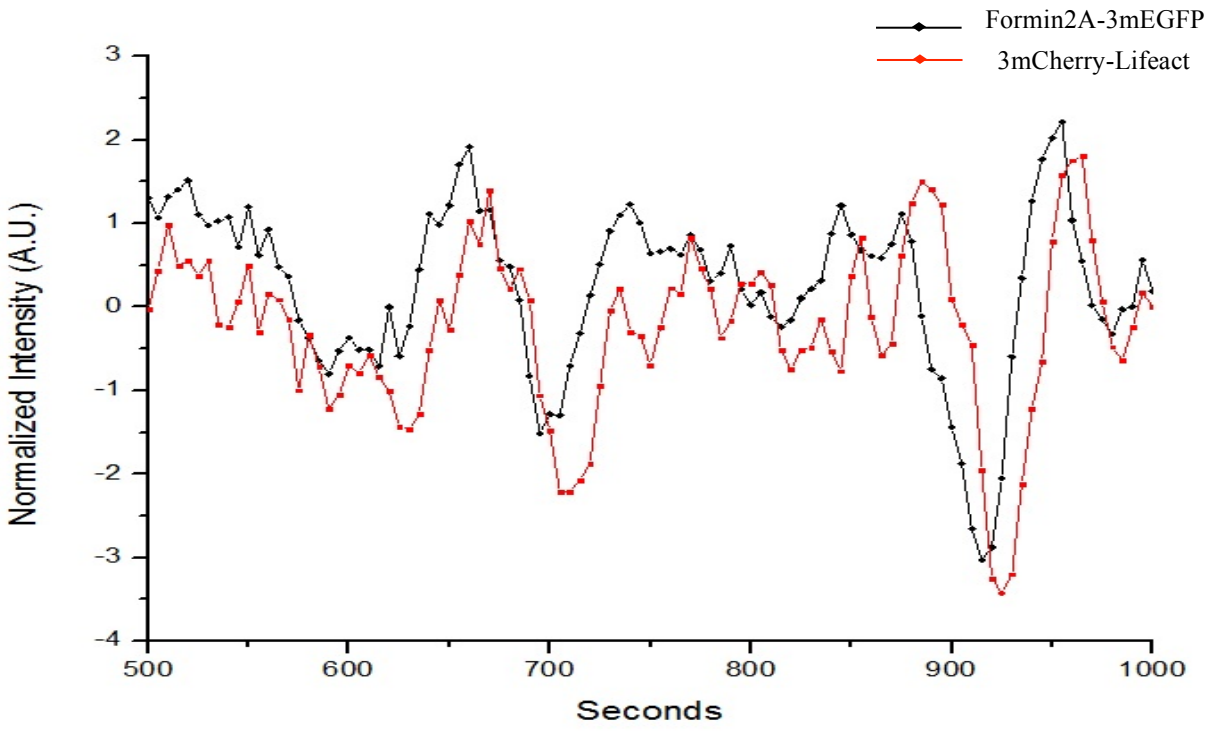

Figure 16: Zoom of the normalized intensity of Formin2A-3mEGFP and 3mCherry-Lifeact over time at the cell tip. (1500-2000 second time frame from Figure 10)

These two figures confirm that the fluorescence intensity, like the formin2A and VAMP, varied rapidly over time as shown in Figure 15. The formin2A (black) appeared to have more extreme positive fluctuations, often peaking higher than those recorded for Lifeact (red). However, the Lifeact seemed to have more extreme negative fluctuations, where it often fell lower than the formin2A. These results also show that the formin2A and the F-actin (Lifeact) appear to be fluctuating at different times. Visually, it appeared that the formin2A was fluctuating before the F-actin. However, it could not be confirmed using these graphs. In order to determine the exact temporal relationship between formin2A and F-actin, the intensities of the two fluorescent tags over all time points were compared to one another. Using another program in Matlab the time difference corresponding to the maximum correlation coefficient between the

two signals was determined by keeping one signal fixed and shifting the other one for each time point. A time difference close to 0 indicates that the signals are fluctuating in phase. . The average result of all 6 cells tested can be seen below in Figure 17.

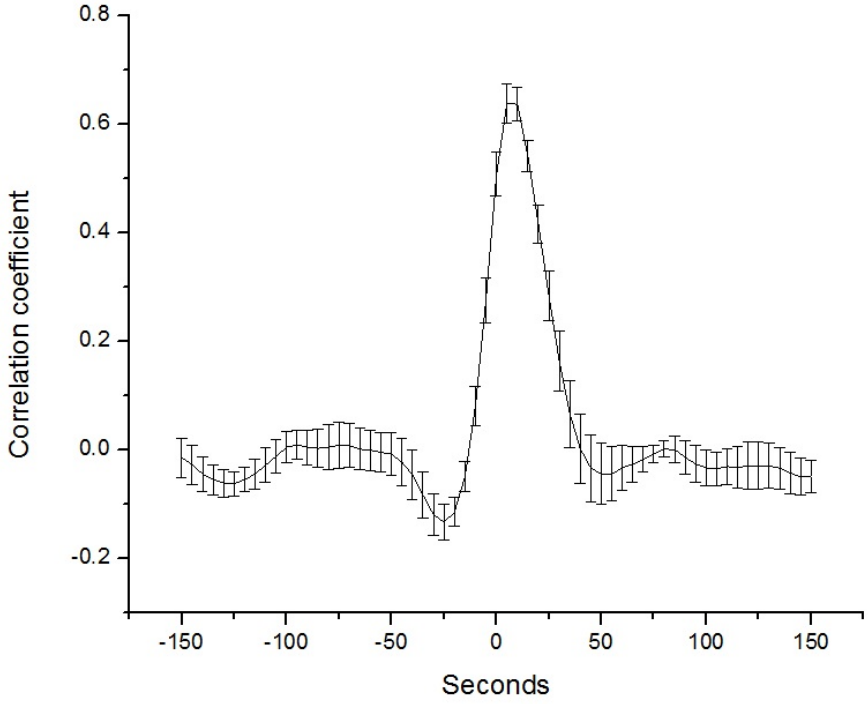

Figure 17: Cross-correlational analysis of Actin vs. Formin2A phase. N=6; error bars are SE of the mean.

As shown earlier in the formin2A and VAMP cross-correlational analysis, the graph is showing the correlation coefficient values for each time shift, with a range of -150 to 150 seconds. The maximum correlation coefficient shows a time shift of 5-10 seconds, indicating that LAMC and formin2A fluctuate at different times at the cell tip during polarized growth. Since the 3mCherry fluorescence is the fixed value in the Matlab program, a negative maximum correlation coefficient means that the 3mCherry precedes the 3mEGFP, and vice versa. The

maximum correlation coefficient in Figure 17 is shown in the positive second range, which indicates that formin2A fluctuated before F-actin.

5.5 RabA21 and Formin2A Localize to the Same Region

In order to test the relationship between formin2A and RabA21, a pre-existing Formin2A-3mEGFP moss line was transformed with a 3mCherry-RabA21 construct using the PEG mediated protocol. Two promising lines were screened out of this transformation, and it was found to express both fluorescent markers (Appendix B). A line was considered good if both fluorescent markers were visibly expressing, and if the gains measured for each color channel was between 700 and 900. In addition, all of the cells tested should be expressing at similar levels. Using confocal microscopy to screen the two lines (database numbers 836 and 837), it was found that RabA21 and Formin2A localize to the same apical region of the caulonemal cell (Figure 18).

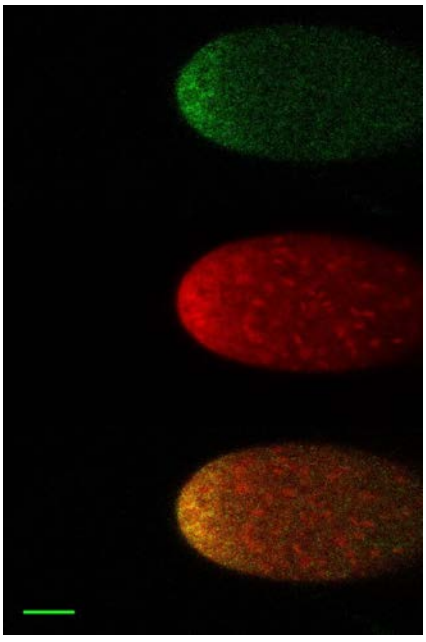

Figure 18: Localization of RabA21 and Formin2A at the tip of a growing caulonemal cell. Images of one transgenic line expressing Formin2A-3mEGFP (upper panel) + 3mCherry-

RabA21 (middle panel) acquired by confocal microscopy. The merged image is shown in the lower panel with Formin2A in green and RabA21 in red. Scale bar = 5 µm

The cell shown in the above figure displays formin2A and RabA21 expression at the tip of the cell. The formin2A shows a slightly faint spot. The RabA21 fluorescence is showing a similar spot at the tip, in addition to fluorescently marked masses in the cell shank, likely organelles. The merged picture shows a large yellow spot where the two fluorescent tags overlap. This indicates that the two are localizing to the same apical region of the cell. The line determined to be the best for testing was line 4. It had the two fluorescent markers expressing, with gains between 700 and 900. All cells tested were expressing the markers at similar levels, indicating homogenous lines.

5.6 CLONING OF 3MCHERRY-VAMP IN A PTKUBIGATE DESTINATION VECTOR

In order to characterize the relationship between vesicles and F-actin, I attempted to generate a line expressing simultaneously 3mEGFP-Lifeact and 3mCherry-VAMP. However, none of the transformations of a pre-existing 3mEGFP-Lifeact line (Vidali et al.) with a 3mCherry-VAMP insert on the pTHUbigate destination vector were successful. This is likely because the 3mEGFP-Lifeact was made using the same destination vector. Due to homologous recombination, the two constructs can compete for the same locus (Pp108 locus) in the DNA. This can cause one of the constructs to not be expressed in the transformed plant. For this reason, the 3mCherry-VAMP was inserted in the pTKUbigate destination vector, which targets a different locus (a redundant copy of the ARPC2 gene) than the pTHUbigate. This means that there would be no competition, and both constructs can be fully expressed (Bezanilla).

Using amplified entry clones containing 3mCherry and VAMP, respectively, and the destination vector pTKUbigate, a LR reaction was performed, in order to combine the two elements. After transformation of *E. coli* with the LR reaction products, four expression clones were screened. In order to determine whether the two elements were correctly inserted in the destination vector backbone, a digestion reaction was performed using two restriction enzymes: NheI and AflII. These were picked because of the location of the corresponding restriction sites on the plasmid, with two restriction sites flanking the insert and one being in the middle of the insert. As a result of a digestion with NheI and AflII, three fragments can be expected with the following sizes: 1095, 4220, and 8660 bp. A virtual construct of the plasmid with these restriction sites was created in Geneious, and can be seen below in Figure 19.

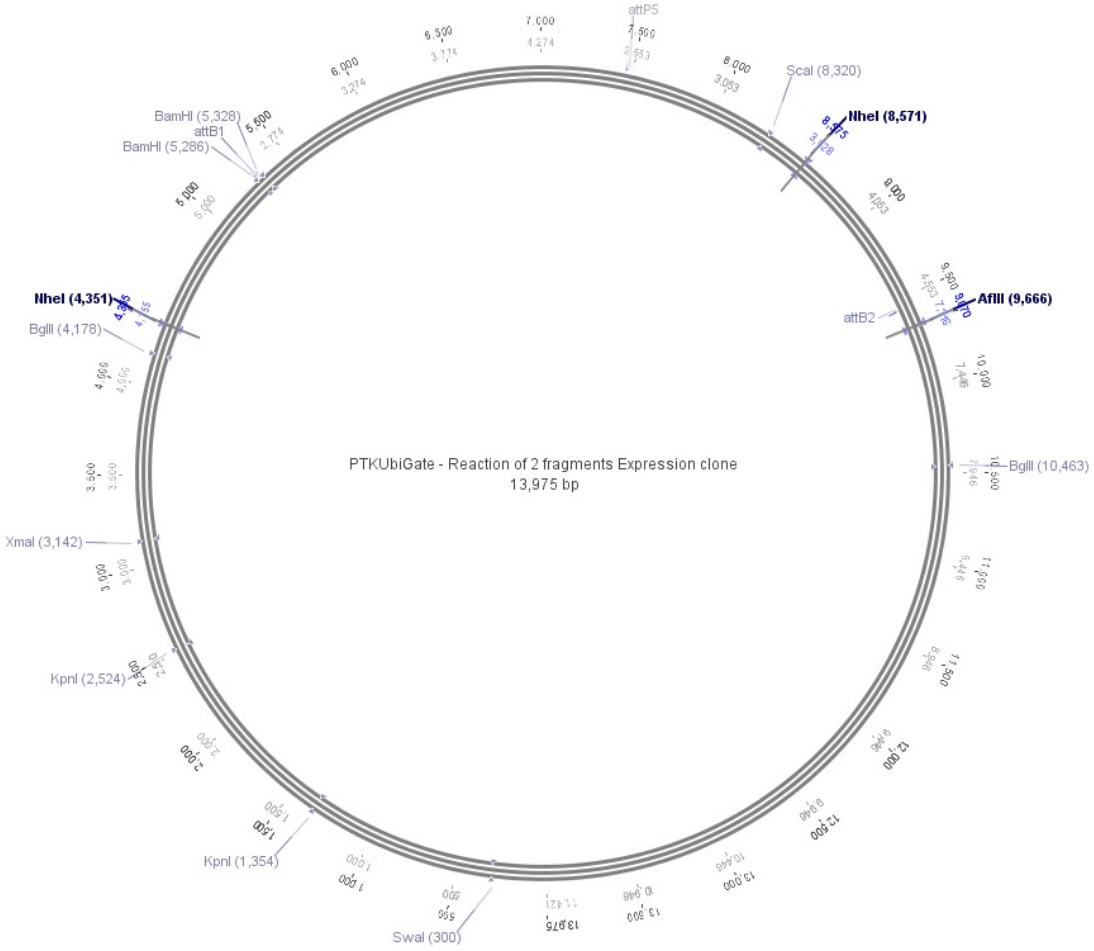

Figure 19: Virtual construction of the expression clone 3mCherry-VAMP in the pTKUbigate destination vector backbone. Restriction sites of NheI and AflII are highlighted in dark blue.

The products of the digestion reaction were analyzed by electrophoresis in agarose gel. A picture of the gel can be seen below in Figure 20, with a ladder on the left to help determine the fragment sizes.

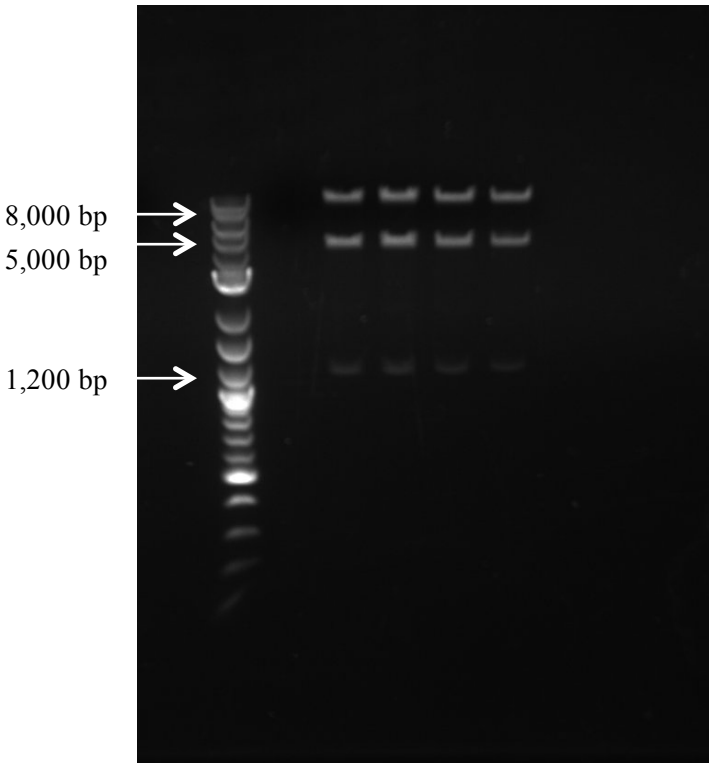

Figure 20: Digestion profile of the four expression clones 3mCherry-VAMP in the pTKUbigate destination vector backbone.

Based off the reference ladder, the profile of the digestion product is consistent with the expected fragment numbers and sizes, which indicates that all four expression clones had been correctly assembled. The two expression clones that had the highest DNA concentration in the mini prep were chosen to be amplified by maxi prep and transformed into the pre-existing moss 3mEGFP-Lifeact line (Vidali et al.). The transformation was successful, and a visual of the stably transformed plants from this can be seen below in Figure 21.

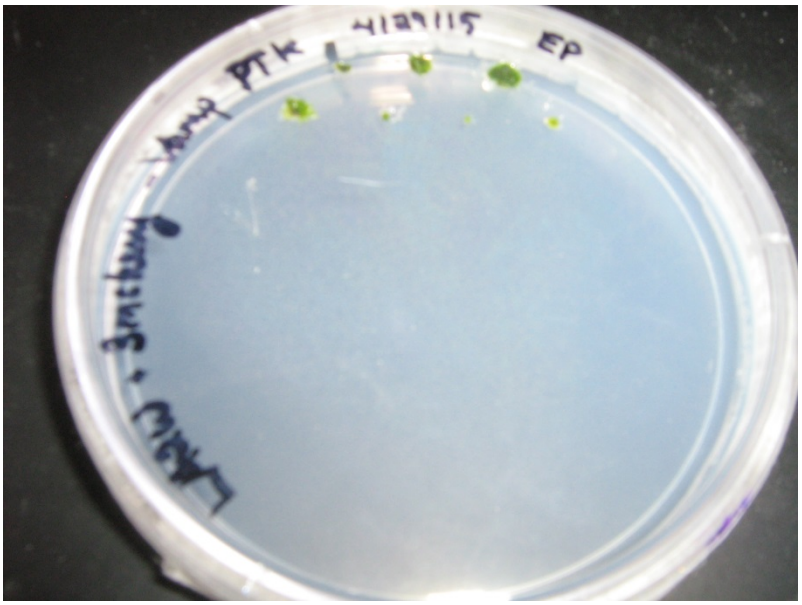

Figure 21: Stable transformed transgenic line expressing 3mEGFP-Lifeact + 3mCherry-VAMP

6 DISCUSSION

The overall purpose of this project was to examine the relationships between a class II formin (formin2A) and other cellular components during polarized growth. Specifically, the purpose was to test the Furt et al. 2013 active polarized growth model, which states that vesicles actively organize the actin network at the cell tip (Furt et al.). The results from this project were expected to help support the active model. According to the model stated previously, I hypothesized that the formin2A would be in phase with the VAMP, and would also precede the Lifeact. I indeed found that formin2A co-localized with VAMP and fluctuated at the same time. This indicates that there is an association between formin2A and vesicles, for which VAMP is a marker. I also showed that formin2A co-localized with the F-actin probe Lifeact, and fluctuation testing showed that formin2A anticipated the Lifeact by around 5-10 seconds.

These results support the lab model for polarized growth in *P. patens*, because VAMP is a vesicle marker, and VAMP co-localized and fluctuated in phase with formin2A. This implies that they are present on the same compartment, such as a vesicle. This is consistent with previous studies, which showed that formin2 co-localized with tagged vesicles in mouse oocytes (Schuh). The same study also showed evidence that the vesicles were organizing the actin network in the oocyte. Class II formins have also been shown to organize endomembranes in fungi and metazoans (Cvrckova et al.). In addition to the formin2A and VAMP results, I showed that formin2A preceded the Lifeact signal. Myosin was also shown to precede Lifeact in a previous study (Furt et al.). This evidence combined with the results shown previously demonstrates that myosin, VAMP (vesicles) and formin2A localize to the same area, and all precede actin. The vesicles anticipate the Lifeact (F-actin), not the other way around.

Some results that were not expected were the cross-correlation results for the formin2A and Lifeact (actin probe) line. Previous literature has cited that myosin fluctuates in phase with VAMP, and precedes actin by 18.6 seconds at the apex of the moss cell during tip growth (Furt et al.). Results from the current project showed that formin and VAMP fluctuate in phase. Therefore, it was expected that the formin would precede the Lifeact by the same amount of time as the myosin had previously. However, the results showed that the formin preceded the Lifeact by 5-10 seconds.

One possibility is that due to formin2A and F-actin interacting very closely when elongating actin filaments, the fluorescent markers used to tag the proteins may have interfered with proper actin filament elongation. Because formin2A works as a dimer that rings the actin filament, it is possible that one or both of the fluorescent tags on the proteins are interfering partially with the process of the actin nucleation. If the Lifeact tag is blocking the hole in the

middle of the formin2A dimer ring, it could interfere with the process and create unusual results. Another alternative is that the fluorescent tag on either the formin or the Lifeact creates a slight conformational change to either protein. If this is the case, it does not appear to have a strong negative effect on the plant and its growth. If there was a strong negative impact, the plant or its growth should show a phenotypic effect. However, a slight conformational change could affect the formin/actin interaction process enough that it causes the anomalous results that were seen during testing.

Another possibility is that the transgenic line created with the tagged formin2A may have interfered with the actin regulation. The line used could be overexpressing formin2A with a fluorescent tag, which could have caused a problem with the actin nucleation and elongation. One way to test this proposal would be to transform the pre-existing 3mEGFP-Lifeact line (Vidali et al.) with a Formin2A-3mCherry construct. However, the formin2A in the construct would be under the control of an inducible promotor. This means that until the Formin2A-3mCherry is induced, the formin2A would not be overexpressed and the 3mEGFP-Lifeact would show the normal actin networks. Once the Formin2A-3mCherry is induced, the plant can be examined under either confocal or TIRF microscopy to see if there is a significant difference in the actin networks. If there is, then that is indicative that overexpressing formin2A is at least partially responsible for the anomalous time shift between formin2A and F-actin seen in this project.

There are several elements that can be examined in future studies to further validate our model. First, if myosin XI and formin are both synchronized with vesicles, I expect that both molecules will fluctuate in phase during polarized growth. Due to the studies and project results mentioned earlier in the report, it is known that myosin XI and VAMP co-localize and are in

phase, the same as formin2A and VAMP (Furt et al.). This would indicate that formin2A and myosin XI would co-localize and fluctuate in phase with each other. However, this has not actually been confirmed through imaging. To test this, a functioning formin2A and myosin XI double line should be created. The preferred myosin XI gene used would be myosin XIa. This is because this isoform of myosin XI normally expresses at higher levels than its counterpart myosin XIb (Vidali et al.).

Attempts had been made over the course of this project to create this line, but there were no successfully expressing lines that could be used to test (Appendices A & B). Stable lines were produced, but during screening little to no 3mCherry expression was observed using the confocal microscope. This was consistent through all lines screened. Since the screened lines spanned multiple transformations, it appears unlikely that the lack of 3mCherry expression was due to a faulty transformation. Since there was no problem with the 3mEGFP expression in any screened formin2A/myosin XIa line, it is instead possible that the 3mCherry-Myo XIa knock-in construct was not created properly. A new 3mCherry-Myo XIa construct would probably have to be made in order to make this line in the future. If the results confirm that formin2A and myosin XIa co-localize and fluctuate in phase, then it would show that formin2A and myosin both have a relationship with vesicles, further supporting the lab model.

Another future study would be to test the 3mEGFP-Lifeact+3mCherry-VAMP lines created during this project. While relationships between polarized growth components (e.g. between myosin and actin or myosin and vesicles) have been studied to determine the accuracy of the active model, the results only indirectly support it. In order to directly support this proposed model, lines containing fluorescently tagged actin (Lifeact) and vesicles (VAMP) needs to be tested. Recommended testing would be the fluctuation testing and cross correlational

analysis used to examine both formin relationships studied during the course of this project. Since the main premise of the active model is that vesicles organize the actin system at the growing cell tip, expected results from this line supporting the active model would be the vesicles preceding the actin, similar to the relationships of myosin and formin with actin (Furt et al.). A second type of test to use on this line would be tracking the vesicles by recording movies in total internal reflection fluorescence (TIRF) microscopy, and seeing if they organize actin filaments. TIRF microscopy allows the user to examine small organelles just under the plasma membrane, and at higher resolutions than other microscopes. Expected results from this type of testing would be that actin filaments elongate outwards from the vesicles, showing that the vesicles organize the surrounding actin network during polarized growth.

In conclusion, the project was a successful one. The formin2A and vesicle hypothesis was supported by the results generated from testing transformed moss lines with confocal microscopy. The formin2A and actin hypothesis was only partially supported, because the cross correlational analysis produced anomalous results. Formin2A fluctuated in phase with vesicles at the growing cell tip, in contrast to the formin2A preceding F-actin. In addition to supporting the project hypotheses, the results also indirectly supported the active model of polarized growth recently proposed by the lab. The work done over the course of this project has set a strong foundation for related future studies that could directly support the lab model, as well as shed further light on the cellular component interactions during polarized growth.

7 REFERENCES

Bezanilla, M. (2015). Moss Methods. from http://www.bezanillalab.com/mossmethods.html.

Buchnik, L., Abu-Abied, M., and Sadot, E. (2015). Role of plant myosins in motile organelles: is a direct interaction required? J Integr Plant Biol **57,** 23-30.

Cove, D.J., Perroud, P.F., Charron, A.J., McDaniel, S.F., Khandelwal, A., and Quatrano, R.S. (2009). The moss *Physcomitrella patens*: a novel model system for plant development and genomic studies. Cold Spring Harb Protoc **2009,** pdb emo115.

Cvrckova, F. (2012). Formins: emerging players in the dynamic plant cell cortex. Scientifica (Cairo) **2012,** 712605.

Cvrckova, F. (2013). Formins and membranes: anchoring cortical actin to the cell wall and beyond. Front Plant Sci **4,** 436.

Cvrckova, F., Oulehlova, D., and Zarsky, V. (2015). Formins: Linking Cytoskeleton and Endomembranes in Plant Cells. Int J Mol Sci **16,** 1-18.

Ebine, K., Fujimoto, M., Okatani, Y., Nishiyama, T., Goh, T., Ito, E., Dainobu, T., Nishitani, A., Uemura, T., Sato, M.H., Thordal-Christensen, H., Tsutsumi, N., Nakano, A., and Ueda, T. (2011). A membrane trafficking pathway regulated by the plant-specific RAB GTPase ARA6. Nat Cell Biol **13,** 853-859.

Furt, F., Liu, Y.C., Bibeau, J.P., Tüzel, E., and Vidali, L. (2013). Apical myosin XI anticipates F-actin during polarized growth of *Physcomitrella patens* cells. Plant J **73,** 417-428.

Harris, S.D. (2008). Branching of fungal hyphae: regulation, mechanisms and comparison with other branching systems. Mycologia **100,** 823-832.

Henty-Ridilla, J.L., Li, J., Blanchoin, L., and Staiger, C.J. (2013). Actin dynamics in the cortical array of plant cells. Curr Opin Plant Biol **16,** 678-687.

Hepler, P.K., Vidali, L., and Cheung, A.Y. (2001). Polarized cell growth in higher plants. Annual Review of Cell and Developmental Biology **17,** 159-187.

Li, J.F., and Nebenfuhr, A. (2008). The tail that wags the dog: the globular tail domain defines the function of myosin V/XI. Traffic **9,** 290-298.

Liu, Y.C., and Vidali, L. (2011). Efficient polyethylene glycol (PEG) mediated transformation of the moss *Physcomitrella patens*. J Vis Exp **50,** DOI 10.3791/2560.

Lodish, H., Berk, A., Zipursky, S., Matsudaira, P., Baltimore, D., Darnell, J. (2000). Molecular Cell Biology. (New York: W. H. Freeman).

Maravillas-Montero, J.L., and Santos-Argumedo, L. (2012). The myosin family: unconventional roles of actin-dependent molecular motors in immune cells. J Leukoc Biol **91,** 35-46.

Menand, B., Calder, G., and Dolan, L. (2007). Both chloronemal and caulonemal cells expand by tip growth in the moss *Physcomitrella patens*. J Exp Bot **58,** 1843-1849.

Palanivelu, R., and Preuss, D. (2000). Pollen tube targeting and axon guidance: parallels in tip growth mechanisms. Trends Cell Biol **10,** 517-524.

Peremyslov, V.V., Prokhnevsky, A.I., and Dolja, V.V. (2010). Class XI myosins are required for development, cell expansion, and F-Actin organization in *Arabidopsis*. Plant Cell **22,** 1883-1897.

Peremyslov, V.V., Klocko, A.L., Fowler, J.E., and Dolja, V.V. (2012). *Arabidopsis* myosin XI-K localizes to the motile endomembrane vesicles associated with F-actin. Frontiers in Plant Science **3,** 184.

Preuss, M.L., Serna, J., Falbel, T.G., Bednarek, S.Y., and Nielsen, E. (2004). The *Arabidopsis* Rab GTPase RabA4b localizes to the tips of growing root hair cells. Plant Cell **16,** 1589-1603.

Rensing, S.A., Lang, D., Zimmer, A.D., Terry, A., Salamov, A., Shapiro, H., Nishiyama, T., Perroud, P.F., Lindquist, E.A., Kamisugi, Y., Tanahashi, T., Sakakibara, K., Fujita, T., Oishi, K., Shin, I.T., Kuroki, Y., Toyoda, A., Suzuki, Y., Hashimoto, S., Yamaguchi, K., Sugano, S., Kohara, Y., Fujiyama, A., Anterola, A., Aoki, S., Ashton, N., Barbazuk, W.B., Barker, E., Bennetzen, J.L., Blankenship, R., Cho, S.H., Dutcher, S.K., Estelle, M., Fawcett, J.A., Gundlach, H., Hanada, K., Heyl, A., Hicks, K.A., Hughes, J., Lohr, M., Mayer, K., Melkozernov, A., Murata, T., Nelson, D.R., Pils, B., Prigge, M., Reiss, B., Renner, T., Rombauts, S., Rushton, P.J., Sanderfoot, A., Schween, G., Shiu, S.H., Stueber, K., Theodoulou, F.L., Tu, H., Van de Peer, Y., Verrier, P.J., Waters, E., Wood, A., Yang, L., Cove, D., Cuming, A.C., Hasebe, M., Lucas, S., Mishler, B.D., Reski, R., Grigoriev, I.V., Quatrano, R.S., and Boore, J.L. (2008). The *Physcomitrella* genome reveals evolutionary insights into the conquest of land by plants. Science **319,** 64-69.

Riedl, J., Crevenna, A.H., Kessenbrock, K., Yu, J.H., Neukirchen, D., Bista, M., Bradke, F., Jenne, D., Holak, T.A., Werb, Z., Sixt, M., and Wedlich-Soldner, R. (2008). Lifeact: a versatile marker to visualize F-actin. Nat Methods **5,** 605-607.

Schuh, M. (2011). An actin-dependent mechanism for long-range vesicle transport. Nat Cell Biol **13,** 1431-1436.

Smith, L.G. (2003). Cytoskeletal control of plant cell shape: getting the fine points. Curr Opin Plant Biol **6,** 63-73.

Tominaga, M., and Nakano, A. (2012). Plant-Specific Myosin XI, a Molecular Perspective. Front Plant Sci **3,** 211.

Trybus, K.M. (2008). Myosin V from head to tail. Cell Mol Life Sci **65,** 1378-1389.

Uemura, T., and Ueda, T. (2014). Plant vacuolar trafficking driven by RAB and SNARE proteins. Curr Opin Plant Biol **22,** 116-121.

van Gisbergen, P.A., and Bezanilla, M. (2013). Plant formins: membrane anchors for actin polymerization. Trends Cell Biol **23,** 227-233.

van Gisbergen, P.A., Li, M., Wu, S.Z., and Bezanilla, M. (2012). Class II formin targeting to the cell cortex by binding PI(3,5)P(2) is essential for polarized growth. J Cell Biol **198,** 235-250.

Vidali, L., and Bezanilla, M. (2012). *Physcomitrella patens*: a model for tip cell growth and differentiation. Curr Opin Plant Biol **15,** 625-631.

Vidali, L., Rounds, C.M., Hepler, P.K., and Bezanilla, M. (2009a). Lifeact-mEGFP reveals a dynamic apical F-actin network in tip growing plant cells. Plos One **4,** e5744.

Vidali, L., Burkart, G.M., Augustine, R.C., Kerdavid, E., Tüzel, E., and Bezanilla, M. (2010). Myosin XI is essential for tip growth in *Physcomitrella patens*. Plant Cell **22,** 1868-1882.

Vidali, L., van Gisbergen, P.A.C., Guerin, C., Franco, P., Li, M., Burkart, G.M., Augustine, R.C., Blanchoin, L., and Bezanilla, M. (2009b). Rapid formin-mediated actin-filament elongation is essential for polarized plant cell growth. Proc Natl Acad Sci U S A **106,** 13341-13346.

Yoo, C.M., Quan, L., Cannon, A.E., Wen, J., and Blancaflor, E.B. (2012). AGD1, a class 1 ARF-GAP, acts in common signaling pathways with phosphoinositide metabolism and the actin cytoskeleton in controlling Arabidopsis root hair polarity. Plant J **69,** 1064-1076.

Zerial, M., and McBride, H. (2001). Rab proteins as membrane organizers. Nature Reviews Molecular Cell Biology **2,** 107-117.

Zigmond, S.H. (2004). Formin-induced nucleation of actin filaments. Curr Opin Cell Biol **16,** 99-105.

APPENDIX A: MATERIALS AND COMPOSITION NEEDED FOR POLYETHYLENE GLYCOL-MEDIATED TRANSFORMATION (LIU AND VIDALI)

Name	Materials
$PPNH_4$	1.84 mM KH_2PO_4 3.4 mM $Ca(NO_3)_2$ 1 mM $MgSO_4$ 2.72 mM Diammonium tartrate 54 µM $FeSO_4.7H_2O$ 9.93 µM H_3BO_3 1.97 µM $MnCl_2.4H_2O$ 0.23 µM $CoCl_2.6H_2O$ 0.19 µM $ZnSO_4.\ 7H_2O$ 0.22 µM $CuSO_4.\ 5H_2O$ 0.10 µM $Na_2MoO_4.2H_2O$ 0.168 µM KI Add 0.7% (w/v) agar for solid medium.
$PPNO_3$	1.84 mM KH_2PO_4 3.4 mM $Ca(NO_3)_2$ 1 mM $MgSO_4$ 54 µM $FeSO_4.7H_2O$ 9.93 µM H_3BO_3

	1.97 µM $MnCl_2.4H_2O$ 0.23 µM $CoCl_2.6H_2O$ 0.19 µM $ZnSO_4$. $7H_2O$ 0.22 µM $CuSO_4$. $5H_2O$ 0.10 µM $Na_2MoO_4.2H_2O$ 0.168 µM KI Add 0.7% (w/v) agar for solid medium.
PRM-B	$PPNH_4$ with 6% (w/v) mannitol and 0.8% (w/v) agar. Add 10 ml 1M $CaCl_2$ to 1 L before pouring plates.
PRM-T	$PPNH_4$ with 6% (w/v) mannitol and 0.6% (w/v) agar. Add 0.5 ml 1M $CaCl_2$ to 50 ml before use.
2% Driselase	Add 4 g of Driselase (Sigma D9515-25G) to 200 ml of 8% (w/v) mannitol. Stir gently for 30 min. at room temperature, incubate 30 min. at 4°C, and stir gently for 5 min. at room temperature. Spin 2,500g for 10 min., discard pellet. Filter with 0.22 µm, and store frozen as 10 ml aliquots. Thaw in a room temperature water bath before use.
MMg	0.4 M mannitol 15 mM $MgCl_2$ 4 mM MES (pH 5.7)
PEG/Ca	4 g PEG4000 3 ml H_2O 2.5 ml 0.8 M mannitol 1 ml 1M $CaCl_2$
W5	154 mM NaCl

	125 mM $CaCl_2$ 5 mM KCl 2 mM MES (pH 5.7)

APPENDIX B: TRACKING SHEET OF ALL TRANSFORMATIONS

Attempted Transformation Line	Time Attempted	Date Attempted	Successful?	If not why
Myo Cterm KI#3+ 3mCherry-RabA53	1	6/26/2014	No	Not enough protoplasts
For7-3mEGFP+ 3mCherry-VAMP	Expanded from Kelsi's master plate			
For7-3mEGFP+ Myo-3mCherry-KI	Expanded from Kelsi's master plate			
Myo Cterm KI #3+3mCherry-RabA53	2	7/3/2014	No	Failed at first Hygro stage
For7-3mEGFP+ LAMC	1	7/11/2014	No	No regenerated protoplasts
For7-3mEGFP+ 3mCherry-RabA21	1	7/18/2014	No	Failed at first Hygro stage
For7-3mEGFP+ LAMC	2	7/25/2014	Yes	
For7-3mEGFP+ 3mCherry-RabA21	2	7/25/2014	Yes	
For7-3mEGFP+ 3mCherry-	1	7/25/2014	Yes	

RabA53				
For7-3mEGFP+ 3mCherry-RabA21	3	9/5/2014	No	Not enough protoplasts
LA2W+ 3mCherry-RabA53	1	9/22/2014	No	Toxic MMG buffer
For7-3mEGFP+ 3mCherry-RabA21	4	9/22/2014	No	Not enough protoplasts
Myo Cterm KI #3+3mCherry-RabA53		Previously expanded by Kelsi		
LA2W+ 3mCherry-VAMP	1	10/9/2014	No	No regenerated protoplasts
For7-3mEGFP+ 3mCherry-RabA21	5	10/9/2014	No	No regenerated protoplasts
LA2W+ 3mCherry-RabA53	2	11/4/2014	No	No regenerated protoplasts
For7-3mEGFP+ 3mCherry-RabA21	6	11/4/2014	No	No generated protoplasts
LA2W+ 3mCherry-VAMP	2	11/13/2014	No	Failed at second Hygro stage
LA2W+ 3mCherry-RabA53	3	11/13/2014	No	Failed at second Hygro stage
LA2W+ 3mCherry-VAMP	3	11/20/2014	No	Master plate lost
LA2W+ 3mCherry-	1	11/20/2014	No	Put on wrong selection media;

RabA53 (pTK)				protoplasts died
LA2W+ 3mCherry-RabA53	4	11/20/2014	No	Failed at first Hygro stage
For7-3mEGFP+ 3mCherry-RabA21	7	11/20/2014	No	Master plate lost
For7-3mEGFP+ 3mCherry-RabA21	8	11/25/2014	Yes	
For7-3mEGFP+ Myo-3mCherry-KI	1	11/25/2014	Yes	
For7-3mEGFP+ LAMC	3	11/25/2014	Yes	
NLS4-3mEGFP-Myo+ 3mCherry-RabA53	1	12/2/2014	Yes	
NLS4-3mEGFP-Myo+ 3mCherry-RabA53	2	1/14/2015	Yes	
LA2W+pTK 3mCherry-VAMP (construct #4)	1	3/18/2015	Yes	
LA2W+pTK 3mCherry-VAMP (construct #4)	2	3/27/2015	Yes	
LA2W+pTK 3mCherry-VAMP (construct #2)	1 for construct #2, 3 for LA2W+pTK 3mCherry-VAMP	3/27/2015	Yes	

LA2W+PTH 3mCherry-VAMP	4	3/27/2015	Yes	

APPENDIX C: TRACKING SHEET OF ALL SCREENING AND FLUCTUATION TESTING

Attempted Transformation Line	Screened?	If not why	Date Screened	Lines Expressing	Holey Slides	Confocal Movies?	Confocal Date	Fluctuation Results Obtained?	Results
For7-3mEGFP+ 3mCherry-VAMP	Yes		6/19/2014	10,19*,28	Yes	Yes	7/1/2014	Yes	Phase=0
For7-3mEGFP+ Myo-3mCherry-KI	Yes		6/24/2014, 7/31/14 and 8/4/14	None					
For7-3mEGFP+ LAMC	Yes		11/10/2014 and 1/13/15	9	Yes	Yes	1/21/2015, 1/23/2015	Yes	Phase=5-10
For7-3mEGFP+ 3mCherry-RabA21	No	Not deemed relevant at that time							
For7-3mEGFP+ 3mCherry-RabA53	No	Not deemed relevant at that time							
Myo Cterm KI #3+3mCherry-RabA53	Screened by Kelsi		N/A	1	Yes	Yes	9/23/2014, 10/7/14, 10/14/14, and 10/29/14	No consistent results	
For7-3mEGFP+ 3mCherry-RabA21	Yes		4/1/2015	4	Yes	Yes	4/8/2015	No consistent results	

For7-3mEGFP+ Myo-3mCherry-KI	Yes		1/30/2015	1*,18	Yes	No. Cherry expression appeared to be overexpressed in both lines			
For7-3mEGFP+ LAMC	Yes		1/13/2015	1	Yes	Yes	1/21/2015	Yes	Phase= 5-10
NLS4-3mEGFP-Myo+ 3mCherry-RabA53	No	No stables expressing							
NLS4-3mEGFP-Myo+ 3mCherry-RabA53	Yes		4/1/2015	2	Yes	No. Screened line was no longer expressing Cherry			